Turkish Journal of Earth Sciences

http://journals.tubitak.gov.tr/earth/

Research Article

Turkish J Earth Sci
(2020) 29: 1049-1072
© TÜBİTAK
doi:10.3906/yer-2003-1

Petrology of the late Triassic mafic volcanic rocks from the Antalya Complex, southern Turkey: evidence for mantle source characteristics during the Neotethyan rifting

Utku BAĞCI[1,*], **Tamer RIZAOĞLU**[2], **Güzide ÖNAL**[3], **Osman PARLAK**[4]

[1]Department of Geological Engineering, Mersin University, Mersin, Turkey

[2]Department of Geological Engineering, Kahramanmaraş Sütçü İmam University, Kahramanmaraş, Turkey

[3]Department of Architecture and City Planning, Maps and Cadastre Program, Mersin University, Vocational School of Technical Sciences, Mersin, Turkey

[4]Department of Geological Engineering, Çukurova University, Adana, Turkey

Received: 05.03.2020 • **Accepted/Published Online:** 14.05.2020 • **Final Version:** 16.11.2020

Abstract: The Antalya Complex in southern Turkey comprises a number of autochthonous and allochthonous units that originated from the Southern Neotethys. Late Triassic volcanic rocks are widespread in the Antalya Complex and are important for the onset of the rifting stage of the southern Neotethys. The studied Late Triassic volcanic rocks within the Antalya Complex are exposed in the southern part of Saklıkent (Antalya) region. They are represented by pillow, massive, and columnar-jointed lava flows with volcaniclastic breccias and pelagic limestone intercalations. Spilitic basalts exhibit intersertal, microlithic porphyritic, and ophitic textures and are represented by plagioclase, pyroxene, and olivine. Secondary phases are characterized by serpentine, calcite, chlorite, epidote, zeolite, and quartz. Based on Zr/Ti vs. Nb/Y ratios, the volcanic rocks are represented by alkaline basalts (Nb/Y = 1.54–2.82). A chondrite normalized REE diagram for the volcanic rocks displays significant LREE enrichment with respect to HREE ($[La/Yb]_N$ = 15.14–19.77). Trace element geochemistry of the studied rocks suggests that these rocks are more akin to ocean island basalt (OIB) and were formed by small degrees (~2–4%) of partial melting of an enriched mantle source (spinel + garnet-bearing lherzolite). The volcanic rocks of the Saklıkent region exhibit similarities to the Late Triassic volcanics of the Koçali Complex in SE Anatolia and the Mamonia Complex (Cyprus) in terms of their geochemical features. All evidence suggests that the Late Triassic alkaline volcanics in Antalya, Mamonia (Cyprus), and the Koçali (Adıyaman) Complexes were formed in an extensional environment at the continent-ocean transition zone during the rifting of the southern Neotethyan Ocean.

Key words: Alkali basalt, seamount, ΔNb, enriched mantle, Neotethys, Antalya Complex

1. Introduction

The Tauride orogenic belt in Turkey is commonly identified as a representative of a continental fragment that had rifted in the Triassic period from a section in northern Africa that was previously known as Gondwana, and then later on followed by another merger and ended with a continental collision in Miocene (Şengör and Yılmaz, 1981; Robertson and Dixon, 1984; Okay et al., 2010). The Taurides contain Cambrian to Tertiary continental and oceanic units (Brunn et al., 1970; Özgül, 1976, 1984; Juteau, 1980; Şengör and Yılmaz, 1981; Ricou et al., 1984; Robertson and Dixon, 1984; Dilek and Moores, 1990; Göncüoğlu, 1997) and are conventionally separated into three parts that are adjoining each other; these are the western, central, and eastern Taurides. One of the key features of the Antalya Nappes, also known as the Antalya Complex, is that the area points northwards and has a V-shaped ridge design, which defines the Isparta Angle found to the west of the Taurides, as shown in Figure 1 (Woodcock and Robertson, 1977; Waldron, 1984). The Antalya Complex, resting tectonically on the Tauride platform, is made up of the volcanic and sedimentary rocks along with the Mesozoic ophiolitic rocks in the Isparta Angle (Poisson, 1977, 1984; Robertson and Woodcock, 1981, 1982; Robertson, 1993). Another unique feature is the allochthonous units found in the Isparta Angle. The emplacement of these units occurred during the Late Cretaceous and Paleocene-Eocene periods. According to Woodcock and Robertson (1982), besides thrusting, transpression and strike-slip tectonics played a crucial role that led to these processes.

It is also evident that Southern Turkey is transected by two belts of Upper Cretaceous ophiolitic rocks, which extend to northern Syria and Cyprus while intervening offshore of the region (Parlak et al., 2009; Robertson et

* Correspondence: bagciu@mersin.edu.tr

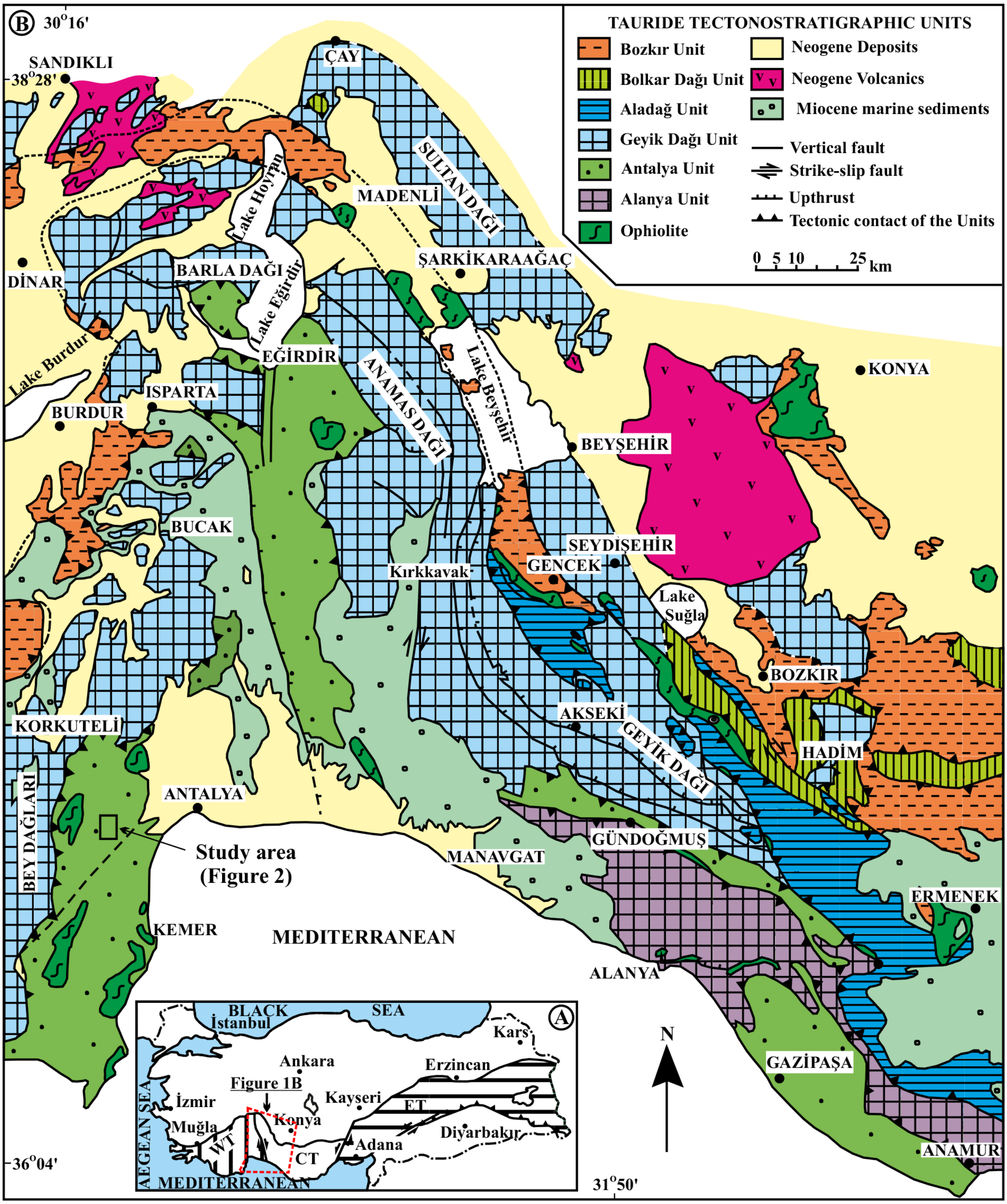

Figure 1. (A) Geographical subdivision of the Tauride belt. WT: western Tauriedes; CT: Central Taurides; ET: Eastern Taurides. (B) Distribution of tectonostratigraphic units in the area between Western and Central Taurides (simplified from Özgül, 1984; Andrew and Robertson, 2002). The location of Figure 2 is indicated.

al., 2012). The belt on the north originates from the Berit ocean, which was found between the Malatya-Keban platform located in the north and Bitlis and Pütürge continental units in the south, comprised of the İspendere, Kömürhan, Göksun, Killan, Guleman ophiolites, and the Berit metaophiolite. The southern belt originating from the Southern Neotethys, on the other hand, is made of the Baer-Bassist ophiolite in northern Syria, Amanos, Koçali, and Hatay ophiolites, Tekirova in Antalya, and the Troodos ophiolite in Cyprus. The existing geophysical records highlight that there is a submarine connection existing between the Levant and Troodos margin ophiolites via the Latakia Ridge (Ben-Avraham et al., 2006; Roberts and Pearce, 2007; Bowman, 2011).

Studies performed on the Antalya Complex (Robertson and Waldron, 1990; Varol et al., 2007; Maury et al., 2008; Elitok, 2012), the Mersin ophiolitic mélange (Parlak and Robertson, 2004; Tekin et al., 2019), the Bitlis Massif (Perinçek, 1980), the Koçali Complex (Varol et al., 2011; Robertson et al., 2016) in Turkey, the Mamonia Complex in southwestern Cyprus (Lapierre et al., 2007), the Baer-Bassist ophiolites in northern Syria (Delaune-Mayère, 1984; Al-Riyami et al., 2002), the Avdella mélange in Greece (Jones and Robertson, 1991), the Hawasina basin in Oman (Lapierre et al., 2004), the central and southern Greece (Pe-Piper, 1982), Albania (Shallo et al., 1990), and the Dinarides in Serbia (Robertson and Karamata, 1994) documented Permo-Triassic volcanisms associated with the rifting of the Neotethyan oceanic basins.

The well-preserved Triassic volcanism associated with rifting in the Southern Neotethys is important for the tectonic evolution of the Mediterranean during the Mesozoic (Robertson, 1998, 2002; Robertson et al., 2004, 2012, 2016). The common features of the Triassic volcanic rocks in the Antalya Complex include within-plate basalts or transitional midocean ridge-type basalts (Robertson and Waldron, 1990; Varol et al., 2007; Maury et al., 2008; Elitok, 2012). Comparison of the Triassic volcanism in terms of mantle source characteristics, degree of partial melting, and their geological settings is critical to better understand the rifting processes in the Southern Neotethys as well as the tectonic processes of the Eastern Mediterranean region.

The aim of this study is (a) to present the petrographical and whole-rock geochemical data of the Triassic volcanic rocks from the Saklıkent region in the Antalya Complex, (b) to discuss mantle source characteristics of the Triassic volcanisms of the Antalya as well as the Mamonia and Koçali Complexes, and (c) to compare and interpret their evolution in the Eastern Mediterranean tectonic frame.

2. Geological setting

The Tauride belt in southern Turkey includes a number of tectonostratigraphic units on the basis of their (a) ages, ranging from Cambrian to Tertiary, (b) distinct stratigraphy and rock assemblages, and (c) tectonic setting (Blumenthal, 1963; Özgül, 1971, 1976; Brunn et al., 1971; Özgül and Arpat, 1973). These units are called the Bolkardağı, Aladağ, Geyikdağı, Alanya, Bozkır, and Antalya Units (Figures 1a and 1b) (Özgül and Arpat, 1973; Özgül, 1976).

Allochthonous rock assemblages in the Antalya bay were first described and named as the Antalya nappes by Lefèvre (1967), Antalya unit (Özgül, 1976), or Antalya Complex (Robertson and Woodcock, 1980, 1982). Later, Brunn et al. (1971) separated the Antalya nappes into three tectonic units that include the upper nappe, middle nappe, and lower nappe identified as the Tahtalıdağ unit, Alakırçay unit, and Çataltepe unit, respectively. Lastly, Şenel et al. (1992, 1996) defined the same units in ascending order as Çataltepe nappe, Alakırçay nappe, Tahtalıdağ nappe, and Tekirova ophiolite nappe. Within the Çataltepe nappe are the Upper Triassic to Upper Cretaceous sedimentary rocks, which include radiolarites, reefal limestones, marls, cherts, flysch, and a shale unit with blocks (Şenel et al., 1992, 1996). The Alakırçay nappe is mainly composed of Middle to Upper Triassic pelagic sediments (radiolarian cherts, pelagic limestones, marls, and shales) associated with basaltic pillow lavas. This unit is in turn unconformably overlain by a flyschoidal with various blocks of Upper Cretaceous age (Şenel et al., 1992, 1996). The Tahtalıdağ nappe is represented by platform-type carbonate rocks from Cambrian to Late Cretaceous (Şenel et al., 1992, 1996). Tekirova ophiolite nappe includes ophiolitic mélange at the bottom, which is tectonically overlain by oceanic lithospheric remnants from mantle tectonites to basaltic volcanics.

The Anisian-Norian (Middle-Upper Triassic) volcanic rocks have a wide-spread outcrop in the Alakırçay formation (Juteau, 1975), Alakırçay Group (Şenel et al., 1981), or Alakırçay unit (Yılmaz, 1984) within the Antalya Complex. The volcanic rocks have a lateral and vertical transition to plant-bearing sandstone, shale, radiolarite, chert, and Halobia-bearing micritic limestones. The volcanics are represented by well-preserved lava flows, basaltic pillow lavas, hyaloclastites, and tuffs (Juteau, 1975). The Middle-Upper Triassic units have been classified into different formations based on rock types and facies (Figure 2). The radiolarite and chert-bearing unit is named the Tesbihli formation; Halobia-bearing limestones are included in the Gökdere formation; pillow lava-bearing unit is named the Karadere formation; and the sandstone-shale unit is called the Çandır formation (Şenel et al., 1992, 1996) (Figure 2).

3. Field relations and petrography

The studied volcanic rocks within the Antalya Complex are exposed in the southern part of the Ziyaret Tepe and Çalbalı Dağ around the Saklıkent region (Figures 2, 3a, and 3b). They are represented by pillow, massive, and columnar-jointed lava flows with volcaniclastic breccias and pelagic limestones (Figures 3c–3f).

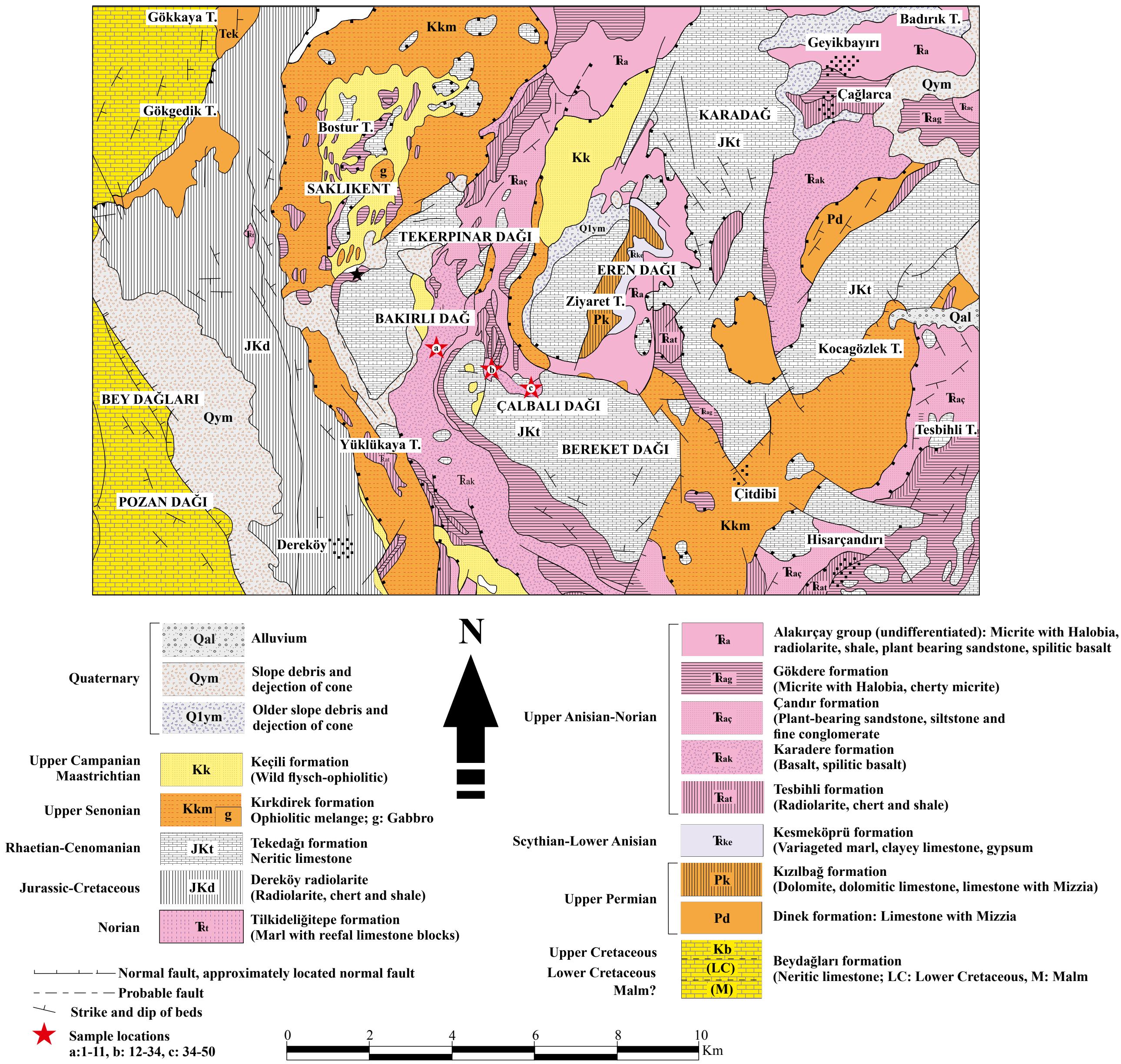

Figure 2. Simplified geological map of the Saklıkent region (from MTA, 2010).

Spilitic basalts exhibit intersertal, microlithic porphyritic, ophitic, and amygdaloidal textures (Figure 4) and are represented by plagioclase, pyroxene, olivine, and small amounts of volcanic glass in the groundmass. Plagioclase and clinopyroxene minerals are observed either as phenocrysts or microliths within the groundmass. The plagioclase forms subhedral phenocrysts (4.5 mm). Some plagioclase crystals show skeletal and sieve textures with their rims partially resorbed by melt (Figure 4). Clinopyroxene displays the euhedral to subhedral outlines (0.5 to 4.3 mm). Anhedral clinopyroxenes appear to be interstitial within plagioclase microlites. Rarely, olivine phenocrysts display subhedral to anhedral shapes and are generally altered to serpentine. Secondary minerals are characterized by calcite, chlorite, epidote, zeolite, and quartz to form the medium to coarse-grained amygdaloidal texture. Calcite also replaces clinopyroxene phenocrysts (Figure 4).

4. Methods

In total, 36 samples were utilized to determine the geochemical features of the Upper Triassic volcanic rocks in the Saklıkent (Antalya) area. The study entailed the trimming of the rock samples to eliminate altered

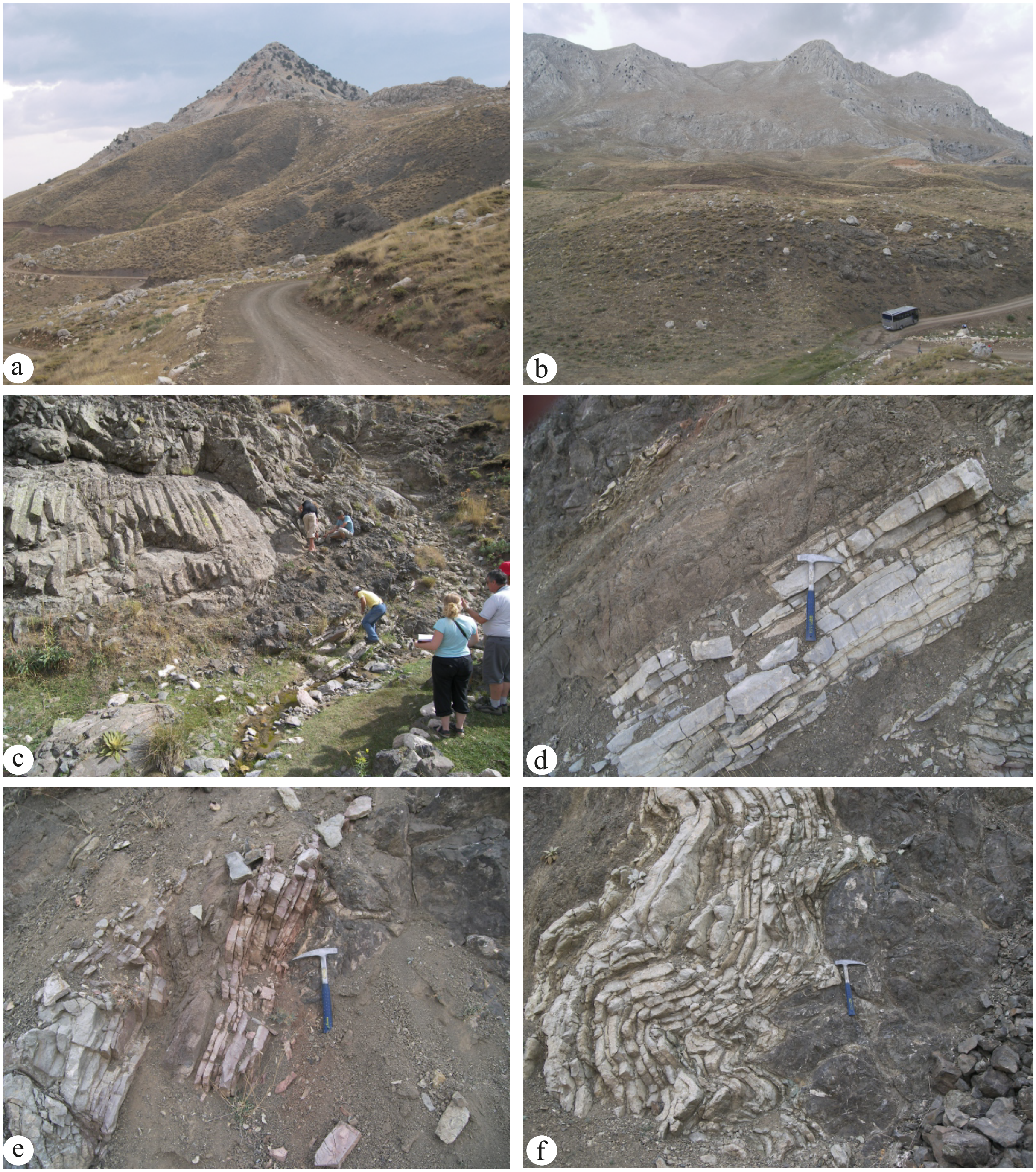

Figure 3. Field views of the volcanic rocks of Saklıkent (Antalya) region. See text for explanation.

surfaces. An agate mill was used for crushing and powdering the collected samples to enable passing a 200-mesh screen. The analyses of whole-rock major and trace elements were carried out at the University of Geneva in Switzerland. In the process, major elements were determined using the X-ray fluorescence (XRF) spectrometer on glass beads merged from ignited powders. Onto this, $Li_2B_4O_7$ was added in a ratio of one to five at a temperature of 1150 °C in a gold-platinum crucible. Analysis of trace elements was performed using the same method on the pressed powder. Another analysis was performed on a subset of six representative samples using inductively coupled plasma mass spectrometry (ICP-MS) for the rare earth elements (REE) in the Department of Mineralogy, University of Geneva.

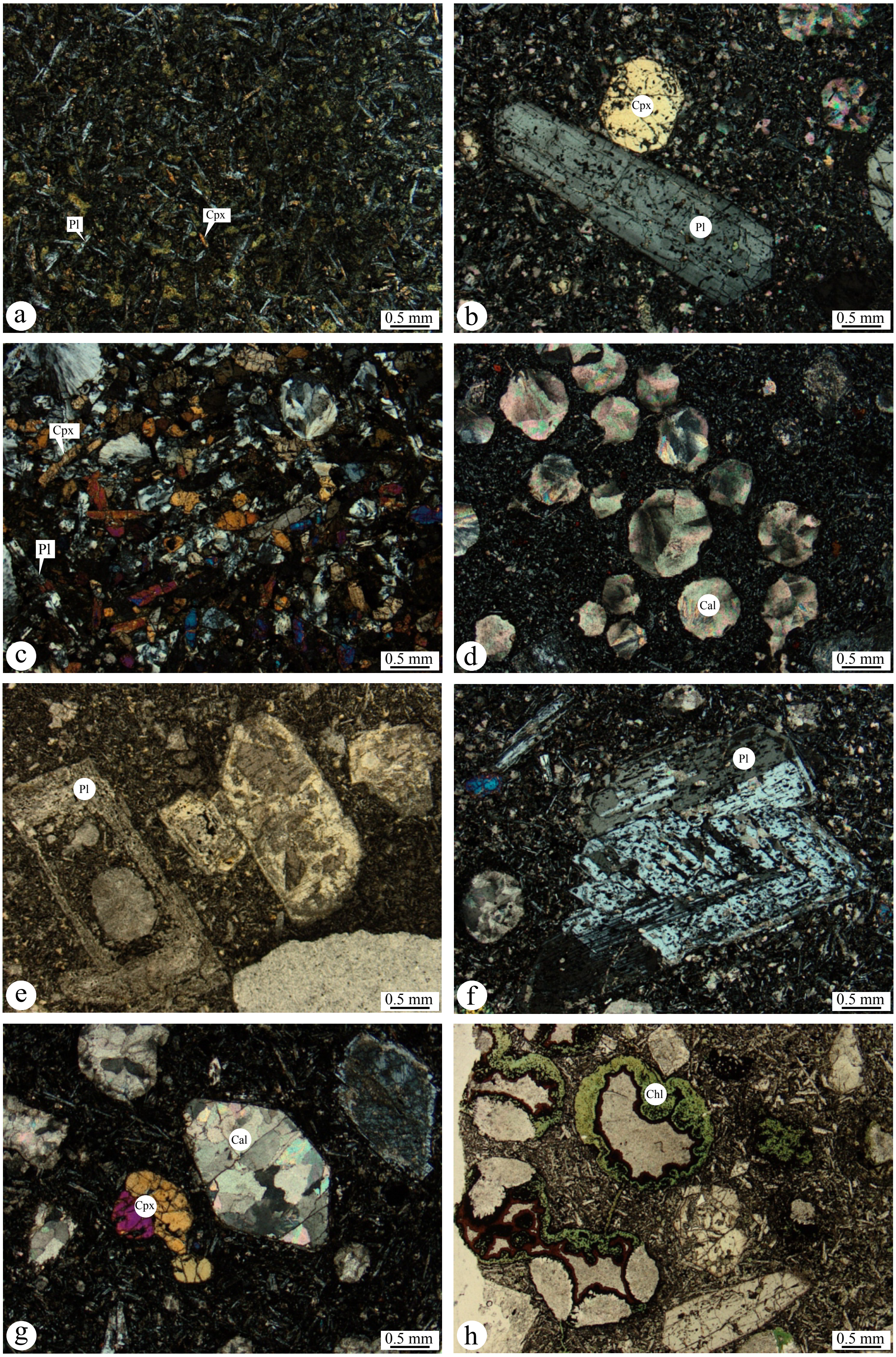

Figure 4. Photomicrographs of the volcanic rocks of Saklıkent (Antalya) region: (a) intersertal, (b) microlithic porphyritic, (c) ophitic and (d) amygdaloidal textures; (e) skeletal and (f) sieve textures in plagioclase; (g–h) calcite and chlorite as secondary minerals. Cross-polarized light (a, b, c, d, f, g), plane-polarized light (e, h). Mineral abbreviation from Whitney and Evans (2010).

Table. Major (wt%) and trace (ppm) element contents of volcanic rocks from the Saklıkent (Antalya) region.

Samples	S 1	S 2	S 3	S 4	S 5	S 9	S 10	S 12	S 13	S 14	S 16	S 17
SiO2	43.54	46.29	39.29	44.99	47.54	31.58	43.87	35.44	32.95	32.41	34.62	35.45
TiO2	3.12	3.51	3.46	3.02	3.32	2.56	3.35	3.05	2.51	2.70	2.71	2.88
Al2O3	12.54	14.03	13.00	13.54	13.89	10.62	14.10	13.73	12.13	11.83	12.37	12.56
FeO	9.08	10.71	8.69	9.72	12.32	8.40	11.32	9.99	8.76	8.34	8.70	10.13
MnO	0.21	0.23	0.23	0.21	0.21	0.18	0.33	0.16	0.18	0.21	0.16	0.17
MgO	2.71	3.68	2.69	3.05	4.43	3.85	3.85	1.52	4.51	4.00	3.33	3.42
CaO	13.90	10.47	13.25	10.27	6.61	20.10	8.86	17.51	18.56	21.72	19.24	17.00
Na2O	3.16	3.48	3.15	5.12	4.06	1.96	3.09	2.41	1.95	1.60	3.20	3.50
K2O	3.19	2.20	3.64	2.13	2.71	1.14	2.19	1.71	0.88	1.06	1.16	1.28
P2O5	0.70	0.77	0.76	0.58	0.63	0.39	1.48	1.42	0.39	0.42	0.41	0.41
Cr2O3	0.00	0.00	0.00	0.00	0.00	0.02	0.00	0.01	0.03	0.03	0.03	0.03
NiO	0.00	0.00	0.00	0.00	0.00	0.01	0.00	0.00	0.01	0.01	0.01	0.01
LOI	7.26	3.91	11.09	6.72	3.66	13.60	6.33	11.82	15.83	14.22	13.41	12.47
Total	99.42	99.28	99.25	99.33	99.38	94.40	98.76	98.78	98.70	98.54	99.33	99.29
Nb	75	85	74	67	69	35	76	43	39	45	43	44
Zr	302	307	297	232	241	183	300	202	214	229	216	170
Y	32	36	29	28	30	17	38	24	17	18	17	23
Sr	313	503	326	172	211	451	810	744	767	496	346	247
U	5	3	5	4	2	4	2	4	2	9	3	6
Rb	33	27	35	29	47	25	24	32	13	14	22	25
Th	14	10	13	11	9	5	7	3	2	6	7	10
Pb	<2	<2	<2	<2	<2	<2	<2	<2	<2	<2	<2	<2
Ga	14	19	14	12	18	13	20	16	10	14	13	14
Zn	106	117	103	100	112	64	132	94	70	71	69	83
Cu	14	13	23	12	10	67	7	27	218	111	71	80
Ni	<2	4	6	3	5	39	7	25	81	69	49	39
Co	25	27	20	22	29	38	23	30	56	48	51	34
Cr	23	44	21	24	18	142	20	57	197	249	205	202
V	226	251	275	232	279	275	182	219	351	309	298	297
Ba	446	546	598	550	795	235	698	883	272	364	256	167
S	86	40	121	41	17	111	1369	218	172	1211	150	83
Hf	3	11	10	9	10	9	7	6	8	5	<1	4
Sc	9	16	7	15	20	<2	21	4	<2	<2	<2	15
As	5	4	5	<3	3	4	5	4	5	5	3	5
La				53.95				50.00				
Ce				105.53				108.39				
Pr				12.15				14.08				
Nd				47.97				61.20				
Sm				9.20				11.83				
Eu				2.63				4.67				
Gd				7.57				9.54				
Tb				1.04				1.17				
Dy				5.90				6.05				
Ho				1.10				1.03				
Er				2.94				2.55				
Tm				0.39				0.31				
Yb				2.43				1.81				
Lu				0.35				0.25				

Table. (Continued).

Samples	S 18	S 20	S 22	S 23	S 24	S 25	S 26	S 28	S 29	S 31	S 33	S 34
SiO2	41.65	34.89	41.74	43.42	44.27	37.83	37.14	37.16	37.44	35.12	39.42	32.30
TiO2	3.02	2.87	2.74	3.48	2.67	2.88	2.00	2.81	2.60	2.50	2.74	1.73
Al2O3	15.20	11.98	15.73	12.47	14.12	12.30	12.64	11.86	11.28	11.31	15.14	10.85
FeO	11.72	8.89	10.58	10.04	11.30	11.47	8.83	9.87	9.63	8.64	9.60	7.70
MnO	0.30	0.42	0.16	0.20	0.17	0.20	0.16	0.25	0.27	0.19	0.17	0.11
MgO	9.35	4.00	5.17	3.59	5.92	2.46	4.09	2.57	3.53	3.12	4.00	3.34
CaO	7.67	18.89	12.17	11.09	9.85	15.88	15.43	17.61	18.06	20.70	15.49	21.02
Na2O	1.74	1.66	2.26	3.00	4.03	2.10	3.75	1.92	1.90	1.77	3.15	0.80
K2O	1.48	2.31	1.66	4.07	1.60	2.33	1.93	2.92	2.50	2.10	1.17	1.96
P2O5	0.68	0.74	0.47	0.71	0.41	0.71	0.33	0.70	0.61	0.57	0.46	0.30
Cr2O3	0.03	0.02	0.01	0.00	0.02	0.02	0.03	0.02	0.03	0.03	0.01	0.05
NiO	0.01	0.01	0.00	0.00	0.01	0.01	0.01	0.01	0.01	0.01	0.00	0.02
LOI	5.48	11.91	6.24	6.77	5.47	11.24	13.17	11.49	10.97	12.90	7.99	18.48
Total	98.33	98.59	98.92	98.84	99.83	99.43	99.51	99.18	98.82	98.96	99.33	98.66
Nb	40	40	42	76	52	53	41	50	45	43	41	28
Zr	152	207	174	277	187	263	178	258	224	228	174	145
Y	26	24	20	33	23	23	18	24	23	21	20	18
Sr	531	431	1137	144	203	420	173	407	380	412	686	278
U	<2	<2	<2	4	2	3	3	3	<2	2	3	<2
Rb	23	34	23	48	25	44	32	44	43	40	22	40
Th	4	5	<2	11	7	10	9	6	3	6	4	4
Pb	<2	<2	<2	<2	<2	<2	<2	<2	<2	<2	<2	<2
Ga	20	16	16	13	18	17	13	15	15	13	16	12
Zn	84	83	79	112	88	102	66	88	82	86	73	101
Cu	51	73	41	7	86	46	50	67	59	54	44	131
Ni	96	37	21	3	46	62	62	46	63	73	22	158
Co	41	46	38	24	34	39	38	36	34	44	38	71
Cr	191	149	57	16	102	140	175	156	189	227	64	339
V	302	253	324	261	381	226	272	222	211	208	333	128
Ba	336	450	735	724	362	387	371	421	359	352	412	261
S	60	1741	854	39	565	83	95	245	123	136	1376	143
Hf	6	2	7	4	9	8	8	8	7	1	4	<1
Sc	34	4	17	10	22	6	7	<2	3	<2	14	<2
As	4	3	4	3	4	4	3	3	5	6	8	4
La									39.69			
Ce									84.67			
Pr									10.58			
Nd									44.06			
Sm									8.79			
Eu									2.40			
Gd									7.20			
Tb									0.95			
Dy									5.24			
Ho									0.94			
Er									2.41			
Tm									0.32			
Yb									1.87			
Lu									0.27			

Table. (Continued).

Samples	S 36	S 38	S 39	S 40	S 41	S 42	S 43	S 45	S 46	S 48	S 49	S 50
SiO2	45.08	40.96	44.61	44.47	44.70	35.22	42.47	40.86	36.68	37.54	44.60	43.45
TiO2	3.52	3.14	3.63	3.43	3.58	2.40	3.30	3.26	2.90	3.69	2.08	2.01
Al2O3	13.63	12.61	13.69	15.13	14.81	13.19	13.02	12.96	11.62	11.85	18.38	17.68
FeO	12.62	8.57	9.17	12.35	12.45	7.09	9.32	9.41	11.31	11.30	7.13	7.05
MnO	0.22	0.22	0.24	0.20	0.20	0.31	0.21	0.32	0.16	0.25	0.14	0.12
MgO	4.45	2.76	3.85	5.19	5.01	4.36	3.79	2.13	3.20	3.00	1.10	1.04
CaO	8.14	14.50	11.46	6.74	7.34	18.70	12.99	12.68	15.47	15.68	10.09	11.23
Na2O	5.01	3.15	3.17	4.66	4.82	1.91	3.21	2.09	1.80	1.97	2.74	2.50
K2O	1.39	3.06	2.81	1.27	1.11	1.46	2.08	4.77	2.77	2.45	3.45	3.57
P2O5	0.69	0.76	0.95	0.69	0.70	0.34	0.82	0.51	0.52	0.64	0.59	0.61
Cr2O3	0.00	0.00	0.00	0.00	0.00	0.01	0.00	0.00	0.00	0.00	0.00	0.00
NiO	0.00	0.00	0.00	0.00	0.00	0.01	0.00	0.00	0.00	0.00	0.00	0.00
LOI	4.84	9.78	5.88	4.17	4.37	13.55	7.34	9.98	12.88	10.82	8.92	9.83
Total	99.60	99.50	99.46	98.31	99.08	98.54	98.57	98.97	99.31	99.19	99.22	99.10
Nb	76	77	82	69	70	40	79	70	62	56	64	63
Zr	270	313	292	224	226	176	286	283	268	274	272	279
Y	33	31	34	30	31	18	31	27	22	24	25	25
Sr	225	374	463	373	378	375	514	350	349	1102	552	570
U	4	11	5	2	2	2	4	5	2	<2	<2	2
Rb	27	40	33	23	20	26	28	41	46	31	65	66
Th	12	11	11	8	10	4	9	10	9	4	7	8
Pb	<2	<2	<2	<2	<2	<2	<2	<2	<2	<2	<2	<2
Ga	20	18	19	20	20	14	17	16	15	15	20	18
Zn	108	106	114	94	96	59	108	98	88	94	82	73
Cu	8	14	12	12	15	92	11	9	10	15	30	30
Ni	4	3	14	6	6	65	<2	2	3	7	16	17
Co	29	31	43	29	28	44	24	31	35	33	18	18
Cr	226	17	143	16	22	89	57	18	16	15	15	133
V	274	236	279	309	325	267	226	314	254	321	152	137
Ba	575	862	588	458	437	303	471	619	405	471	548	553
S	931	250	607	226	120	1471	1147	116	161	165	74	120
Hf	5	5	8	8	7	2	9	3	1	3	8	7
Sc	20	7	13	21	25	<2	13	4	6	8	11	9
As	5	<3	4	5	5	4	5	<3	6	4	7	5
La				54.60				48.77				46.86
Ce				109.08				96.40				90.99
Pr				12.73				11.19				10.50
Nd				50.60				43.84				40.99
Sm				9.83				8.47				7.78
Eu				2.87				2.44				2.32
Gd				8.47				7.26				6.33
Tb				1.15				0.99				0.86
Dy				6.42				5.60				4.88
Ho				1.17				1.03				0.91
Er				3.11				2.77				2.44
Tm				0.42				0.37				0.33
Yb				2.50				2.31				2.08
Lu				0.36				0.34				0.30

5. Geochemistry

5.1. Assessment of alteration

Whole-rock major, trace, and rare earth element data of the volcanic rocks are presented in Table. It is clear that volcanic rocks are characterized by high contents of volatile oxides ($H_2O + CO_2$) varying between 3.66 and 18.48 wt%, which show the presence of variable secondary alteration-related mineral phases, as discussed in the petrography section. Selective major and trace element mobility is expected to occur, mainly in large ion lithophile elements (LILE) during the alteration processes. Major and trace elements are compared against Zr to evaluate the mobility of the elements in Figure 5. As shown, Na, Si, Rb, and Sr indicate that the scattered distribution against Zr is not systematic, highlighting their mobility. Therefore, this points to the idea that selected LIL elements are unreliable indicators when determining petrogenetic relationships. Element mobility during alteration is a well-known process (Hart et al., 1974; Humphris and Thompson, 1978), whereas selected HFS (Ti, Y, Nb) and P element contents against Zr in Figures 5e–5f exhibit linear trends, therefore these elements are relatively immobile and used for rocks classification, petrogenetic interpretation, and tectonic setting (Pearce and Cann, 1973; Floyd and Winchester, 1975; Pearce and Norry, 1979).

5.2. Results

The studied samples are characterized by high TiO_2 (1.73–3.69 wt%), Zr (145–313 ppm), Y (17–38 ppm), and Nb (28–85 ppm) as well as LREE contents (Table). These features may suggest that the studied samples were probably derived from an enriched mantle source. The detailed geochemical features of the samples will be described below. Published data for basic volcanic rocks from the Antalya (Varol et al., 2007; Maury et al., 2008; Elitok, 2012), Mamonia (Cyprus) (Lapierre et al., 2007), and Koçali (Adıyaman) (Varol et al., 2011; Robertson et al., 2016) Complexes will be used together with our results to compare and better understand the magma source characteristics during Southern Neotethyan rifting.

Based on the Zr/Ti vs. Nb/Y ratios, volcanic rocks from the Saklıkent (Antalya) region are represented by alkaline basalts (Nb/Y = 1.54–2.82) in Figure 6 (after Pearce, 1996), in accordance with the Triassic alkaline basalts of the Antalya Complex (Varol et al., 2007; Maury et al., 2008; Elitok, 2012), ocean island basalts (OIB) of the Koçali (Varol et al., 2011; Robertson et al., 2016), and Type-3 alkali basalts of the Mamonia Complex (Lapierre et al., 2007). In contrast, the subalkaline basaltic rocks defined as enriched midocean ridge basalts (E-MORB) from the Koçali Complex (Varol et al., 2011; Robertson et al., 2016), as well as Type 1–2 volcanics from Mamonia (Lapierre et al., 2007) and Antalya (Elitok, 2012) were characterized by lower Nb/Y contents (Figure 6).

Chondrite-normalized REE and N-MORB normalized multielement diagrams for the Late Triassic volcanic rocks studied from the Saklıkent region, together with data from the Mamonia (Lapierre et al., 2007), Koçali, (Varol et al., 2011; Robertson et al., 2016), and Antalya (Varol et al., 2007; Maury et al., 2008; Elitok, 2012) Complexes, N-MORB, OIB, and E-MORB are presented for comparison in Figure 7. The REE concentrations vary from 9.8 to 230 times enrichment compared to chondritic values. These patterns display light rare earth element (LREE) enrichment and heavy rare earth element (HREE) fractionation (La_N/Yb_N = 15.14–19.77), indicating the asthenosphere as a possible origin for enriched mantle source components, exhibiting highly close similarity with the ocean island basaltic units (Sun and McDonough, 1989) (Figure 7a). The alkaline basalts of the Koçali (La_N/Yb_N = 7.0–21.5), Antalya (La_N/Yb_N = 9.3–18.3), and Mamonia (La_N/Yb_N = 4.2–15.2) Complexes are characterized by a similar LREE enrichment (Lapierre et al., 2007; Varol et al., 2007, 2011; Maury et al., 2008; Elitok, 2012; Robertson et al., 2016) (Figures 7c, 7e, and 7g). In contrast, Late Triassic tholeiitic volcanics in Antalya (La_N/Yb_N = 1.1–2.3), Koçali (La_N/Yb_N = 1.0–2.0), and Mamonia (La_N/Yb_N = 0.6–1.6) Complexes exhibit LREE-depleted to flat REE patterns and are more akin to E-MORB (Figures 7c, 7e, and 7g).

In multielement diagrams, all are enriched in HFS, LREE, and middle rare earth elements (MREE) and slightly depleted heavy rare earth elements (HREE) relative to N-MORB (Figures 7b, 7d, 7f, and 7h). Alkaline volcanics from the Koçali, Mamonia, and Antalya Complexes also exhibit similar OIB-type multielement patterns. These rocks have high abundances of HFS in respect to N-MORB. This situation can be explained by enriched mantle melting and/or small degrees of partial melting (Aldanmaz et al., 2000). In contrast, the Late Triassic tholeiitic volcanics in Koçali, Mamonia, and Antalya Complexes exhibit similarities to E-MORB multielement patterns (Figures 7d, 7f, and 7h). The E-MORB is considered to be a result of a higher degree of partial melting of a potentially similar upper mantle source.

5.3. Petrogenesis

In this section, mantle source characteristics of the studied alkaline rocks, as well as published data for the volcanics of the Antalya, Mamonia, and Koçali Complexes that are important for the rifting of the Southern Neotethyan Ocean will be evaluated together. Ratio-ratio incompatible element plots are used in Figure 8 to describe the mantle source regions for Late Triassic volcanic rocks from the Antalya, Mamonia, and Koçali Complexes together with those of normal midocean ridge basalts (N-MORB), ocean island basalts (OIB), and E-MORB. High Sm/Yb vs. Ce/Sm, as well as Zr/Nb vs. Ti/Nb ratios of the studied alkaline Triassic lavas, suggest that they were derived by the melting

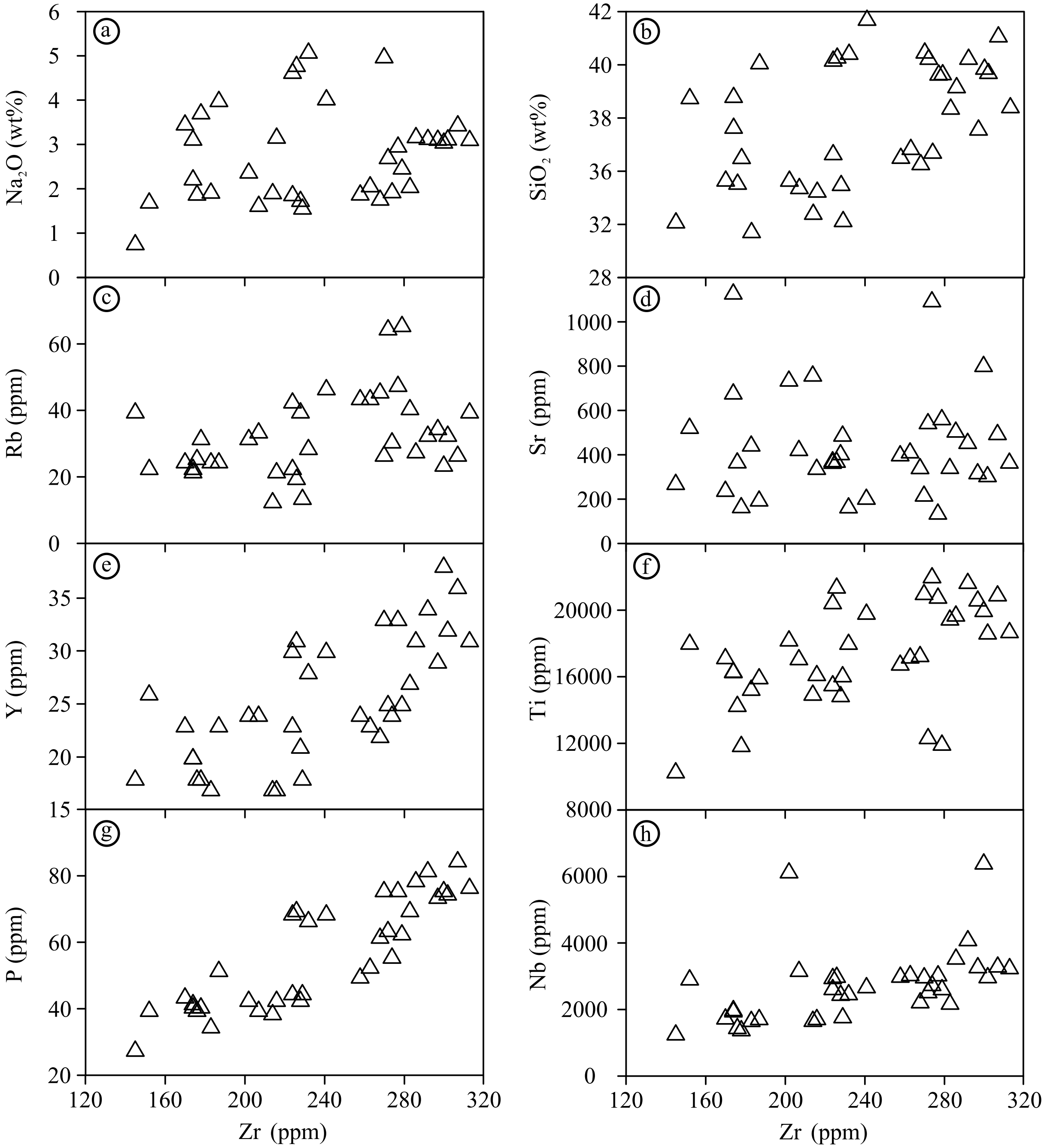

Figure 5. Variations of selected major and trace element contents against Zr for the volcanic rocks in Saklıkent (Antalya) region.

of an OIB-like enriched mantle source, exhibiting close similarity to alkaline basalts of the Koçali, Antalya, and Mamonia Complexes (Lapierre et al., 2007; Varol et al., 2007, 2011; Maury et al., 2008; Elitok, 2012; Robertson et al., 2016). In contrast, the tholeiitic samples from Antalya (Elitok, 2012), Koçali (Varol et al., 2011; Robertson et al., 2016), and Mamonia (Lapierre et al., 2007) are closer to E-MORB and N-MORB (Figure 8), indicating derivation from a mantle source similar to more depleted MORB.

Th/Yb vs. Nb/Yb ratios of the Late Triassic basic volcanic rocks from the study area in Figure 9 (Pearce, 1983; Pearce and Peate, 1995) indicate that these ratios are nearly independent of fractional crystallization and/or partial melting (with dominant crystallization or residual phases of pyroxenes and feldspars), and hence stresses source variations, partial melting, and crustal assimilation (Aldanmaz et al., 2000). Th and Nb are the elements whose fractionation is negligible during the melting of

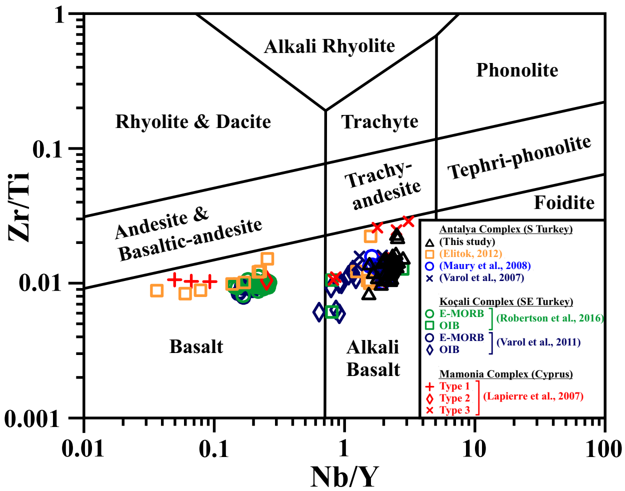

Figure 6. Zr/Ti vs. Nb/Y (after Pearce, 1996) diagram for the volcanic rocks of Saklıkent (Antalya) region. Data for the Antalya Complex are from Varol et al. (2007) and Elitok (2012); data for the Mamonia Complex are from Lapierre et al. (2007); data for the Koçali Complex are from Varol et al. (2011) and Robertson et al. (2016).

peridotitic mantle under upper mantle conditions (e.g., Sun and McDonough, 1989), suggesting that lavas from nonsubduction settings plot along a MORB-OIB array (including almost all midocean ridge and most ocean island basalts). However, subduction processes cause source region metasomatism with enrichment of Th in comparison with Nb (Ta) and therefore in Th/Yb ratios higher than Nb(Ta)/Yb, Th element is generally carried by slab-derived fluids or melts, whereas Ta or Yb elements are not carried by those agents (Pearce, 1983; Tatsumi and Eggins, 1995). Th/Yb ratios relative to Ta/Yb ratios may also be increased by crustal contamination due to higher Th abundances than Ta/Yb in crustal rocks in general (Aldanmaz et al., 2000). The Th/Yb vs. Nb/Yb variation diagram shows that alkaline and tholeiitic lavas display no influence of subduction chemical component (Figure 9). High Th/Yb and Nb/Yb ratios of alkaline Triassic lavas suggest that they were derived from an enriched mantle source and/or generated under low degrees of partial melting, similar to alkaline basalts of the Koçali, Antalya, and Mamonia Complexes (Lapierre et al., 2007; Varol et al., 2007, 2011; Maury et al., 2008; Elitok, 2012; Robertson et al., 2016). In contrast, the tholeiitic samples from the Antalya (Elitok, 2012), Koçali (Varol et al., 2011; Robertson et al., 2016), and Mamonia (Lapierre et al., 2007) are mainly plotted on the E-MORB and to a lesser extent N-MORB field (Figure 9).

The ΔNb parameter (Fitton et al., 1997; Fitton, 2007) has been interpreted as a valuable indicator for relative change of enrichment or depletion. Specifically, ΔNb expresses the excess or deficiency from a reference (ΔNb = 0) separating parallel Icelandic and N-MORB arrays on a logarithmic plot of Nb/Y vs. Zr/Y is expressed (Fitton, 2007). At least 35 of the samples from the Saklıkent region display positive ΔNb values. However, only a single sample had a negative ΔNb value (Figure 10a; Table). ΔNb values for previous studies in Antalya, Mamonia, and Koçali Complexes are characterized mainly by positive values. The parallel lines in Figure 10b define the upper and lower limits of the Iceland data array by Fitton (2007). N-MORB is lack of Nb compared to the primitive mantle (PM), E-MORB, and OIB. The Nb is stored in subducted oceanic crust, possibly in rutile phase, and consequently recycled in the mantle as a source component of OIBs (Fitton et al., 1991; Kempton et al., 1991; Hofmann, 1997; Rudnick et al., 2000; Fitton, 2007). A logarithmic plot of Nb/Y vs. Zr/Y indicates that positive ΔNb values from these regions are compared to a compositional range of Icelandic basalts and plotted along the E-MORB and OIB trend. In contrast, the negative ΔNb values from the Koçali and Mamonia and Antalya Complexes are below the compositional range of Icelandic basalts and show similarity to N-MORB (Figure 10b) (Lapierre et al., 2007; Varol et al., 2007, 2011; Maury et al., 2008; Elitok, 2012; Robertson et al., 2016).

In recent years, trace elements have been widely used in petrogenetic source modeling for deciphering source characteristics in terms of the extent of partial melting and the nature of the mantle source (as enriched or depleted). In modeling, the REE concentration changes during the melting of the depleted MORB mantle (DMM), the primitive mantle (PM), and a speculated enriched mantle (EM) from western Anatolia. Aldanmaz et al. (2000) utilized nonmodal batch melting equations. The elements La and Sm do not experience the significant impact of the variations in the source mineralogy, such as garnet or spinel, in the processes of partial melting because the two elements are incompatible (Aldanmaz et al., 2000). In the La/Sm vs. La diagram, the samples from the Saklıkent area plot close to the melting trend of the enriched mantle (EM) source with a melting degree between ~2 and 4% (Figure 11a), suggesting a mantle source to be enriched in LREE with respect to DMM composition in order to produce alkaline volcanic rocks (Aldanmaz et al., 2000). Alkaline volcanics from the Antalya (with melting degree of ~2%–5%), Koçali (with melting degree of ~2%–10%), and Mamonia (with melting degree of ~2%–10%) Complexes have similar melting trends of the enriched mantle (EM) source (Varol et al., 2007, 2011; Maury et al., 2008; Elitok, 2012; Robertson et al., 2016; Lapierre et al., 2007) (Figure 11a). In contrast, the tholeiitic volcanic rocks of the Koçali, Antalya, and Mamonia Complexes have La/Sm vs. La contents similar to the melting trend of the depleted MORB mantle (DMM) with melting

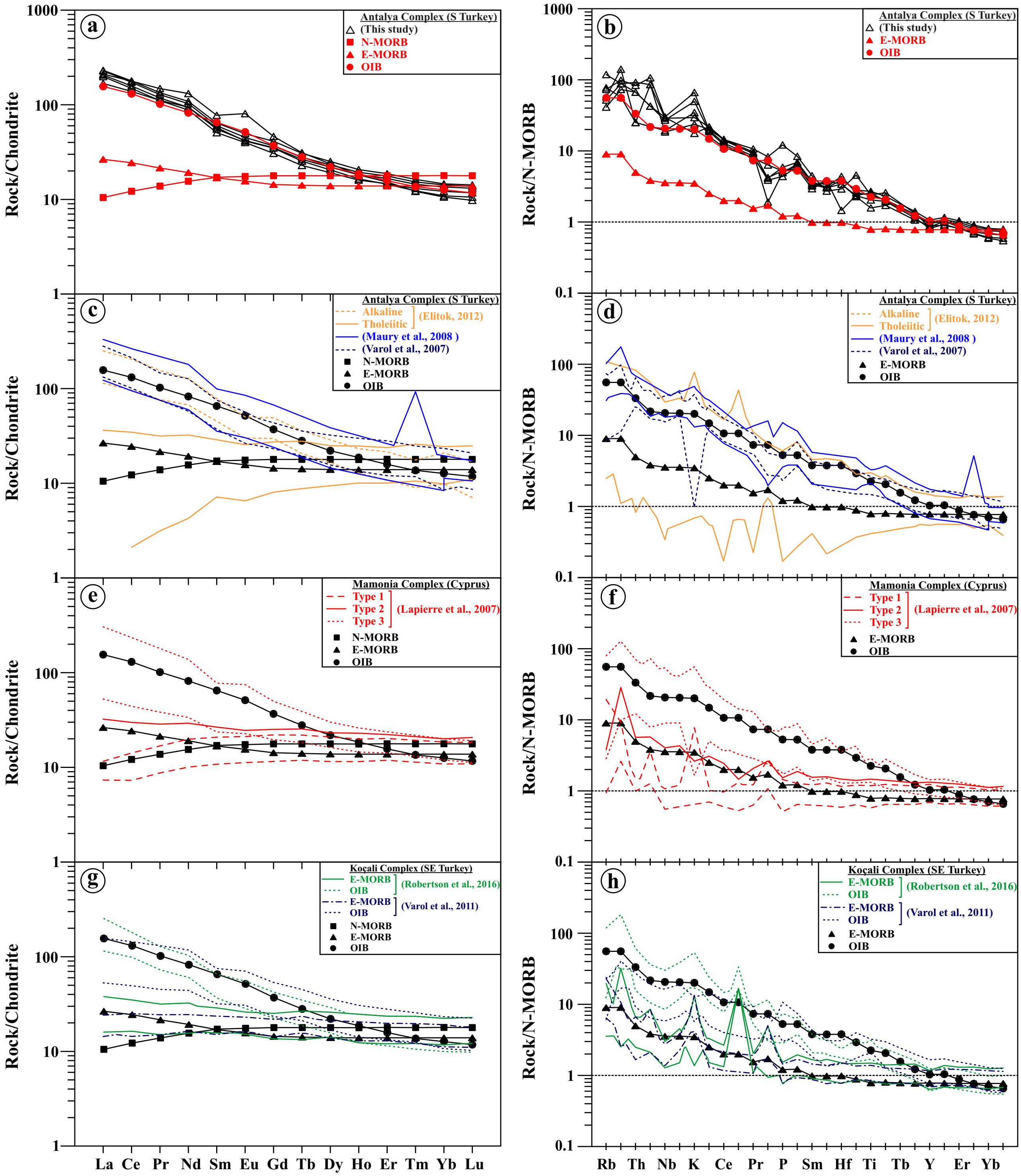

Figure 7. Chondrite-normalized REE (a, c, e, g) and N-MORB normalized spider diagrams (b, d, f, h) for the volcanic rocks of Saklıkent (Antalya) region. Normalizing values are from Sun and McDonough (1989). The data sources and symbols are the same as in Figure 6.

degrees of ~2%–15% for Antalya (Elitok, 2012), ~2%–5% for Koçali (Varol et al., 2011; Robertson et al., 2016), and ~2%–10% for Mamonia (Lapierre et al., 2007) (Figure 11a). Since Yb is not compatible with other minerals like clinopyroxene but is compatible with garnet, the existence of the garnet in the mantle source plays a significant role in controlling the contents of Yb in mantle-derived melts. In the diagram of Sm/Yb vs. Sm, the alkaline volcanic

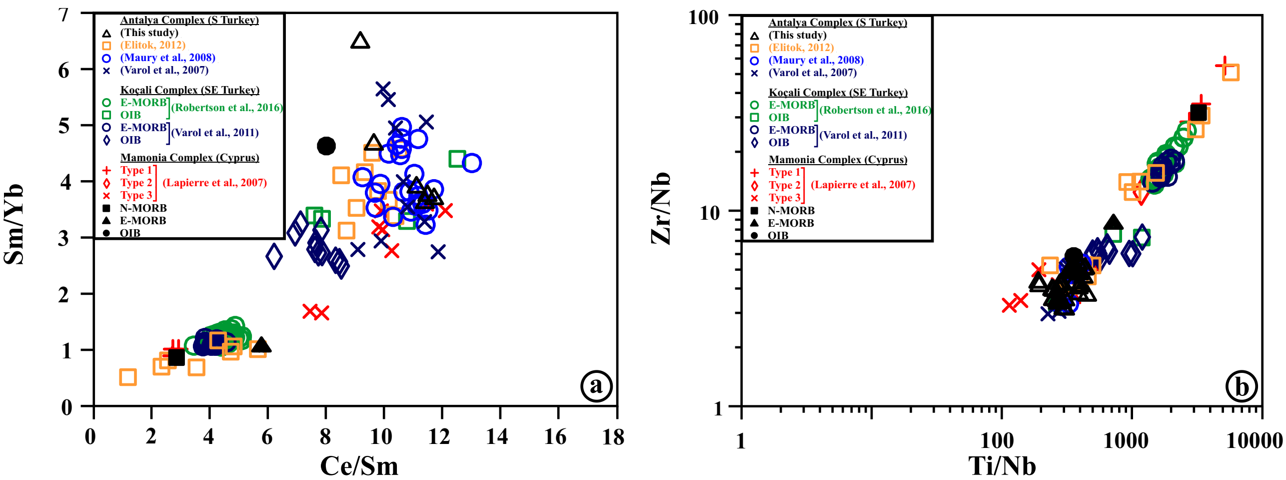

Figure 8. **(a)** Ce/Sm vs. Sm/Yb and (b) Ti/Nb vs. Zr/Nb diagrams for the volcanic rocks of Saklıkent (Antalya) region. N-MORB, E-MORB, and OIB compositions are from Sun and McDonough (1989). The data sources and symbols are the same as in Figure 6.

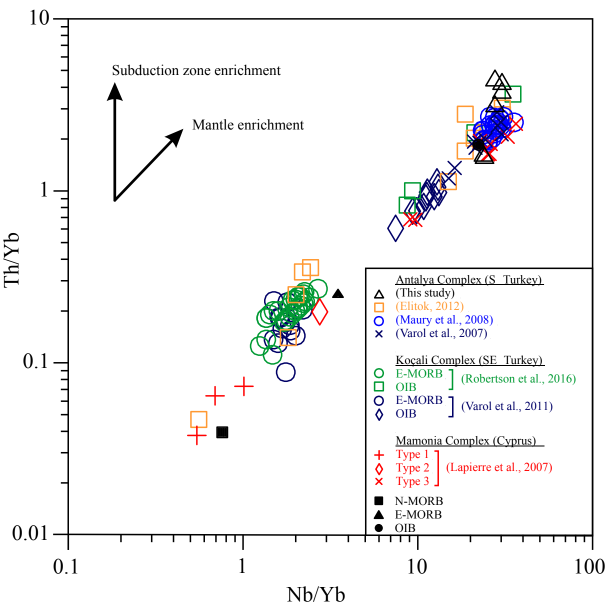

Figure 9. Th/Yb vs. Nb/Yb diagram for the volcanic rocks of Saklıkent (Antalya) region (after Pearce, 1983). The data sources and symbols are the same as in Figure 6.

rocks from Antalya, Mamonia, and Koçali plot in between garnet and spinel-garnet lherzolite melting trajectories, indicating that garnet was residual in their source region (Figure 11b). The tholeiitic volcanic rocks from the Koçali (Adıyaman), Antalya, and Mamonia (Cyprus) Complexes exhibit similarities to E-MORB and plot close to the melting trend of the spinel-lherzolite facies DMM source (Figure 11b). The diagram of Sm/Yb versus La/Sm shows that when the spinel-lherzolite source melts, it results in a horizontal melting pattern lying near the DMM- and PM-type mantle compositions. In contrast, a small degree of partial melting of a garnet-lherzolite source produces melts with higher Sm/Yb ratios than the mantle source (Aldanmaz et al., 2000). The alkaline volcanic rocks from the Saklıkent area plot in between garnet- and spinel-garnet lherzolite melting trends, suggesting that alkaline volcanics involve garnet + spinel mantle mineralogies. The Late Triassic alkaline rocks in Antalya, Koçali, and Mamonia Complexes have similarities with the Late Miocene alkaline volcanic of western Turkey (Aldanmaz et al., 2000). In contrast, the tholeiitic volcanic rocks from the Koçali, Antalya, and Mamonia Complexes plot close to the melting trend of the spinel-lherzolite facies DMM source (Figure 11c).

Tectonic-environment discrimination diagrams (Figure 12) on the basis of immobile trace elements show within-plate affinities for the alkaline volcanics from the Saklıkent area and the Koçali, Antalya, and Mamonia Complexes (Lapierre et al., 2007; Varol et al., 2007, 2011; Maury et al., 2008; Elitok, 2012; Robertson et al., 2016). In contrast, tholeiitic volcanics from the Antalya, the Koçali, and the Mamonia Complexes are plotted between MORB and OIB, suggesting E-MORB characteristics (Lapierre et al., 2007; Varol et al., 2011; Elitok, 2012; Robertson et al., 2016).

6. Discussion and conclusions

It is evident that OIBs and E-MORBs are usually present in widespread continental rifts, midoceanic ridges, and ocean island environments. E-MORB, which is enriched in alkali and incompatible elements relative to N-MORB, is commonly known to have its origin in the volcanic islands such as Iceland, as seen in Figure 11b. At the same time, significant seamounts and some topographically

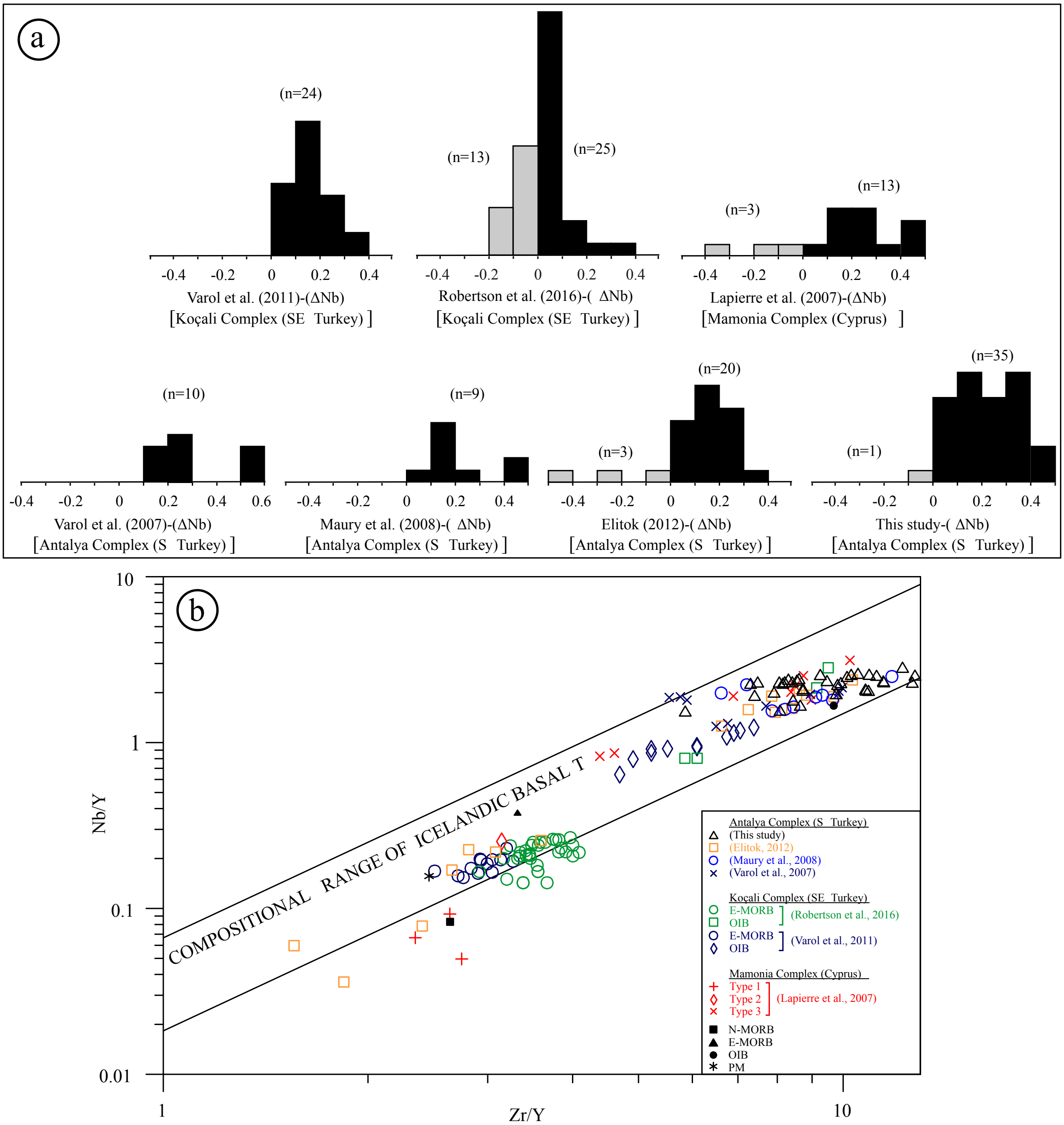

Figure 10. (a) A histogram of ΔNb and (b) Nb/Y and Zr/Y variation diagram for the volcanic rocks of Saklıkent (Antalya) region as well as the Mamonia Complex, the Koçali complex, and the Antalya Complex. The data sources and symbols are the same as in Figure 6. Primitive mantle (PM) composition is from McDonough and Sun (1995), N-MORB, E-MORB, and OIB compositions are from Sun and McDonough (1989).

raised regions near the ocean islands can be observed at the southern Midatlantic ridge and southwest and central Indian ridges (Le Roux et al., 2002; Janney et al., 2005; Murton et al., 2005; Nauret et al., 2006). According to Fitton (2007), OIBs and E-MORBs are consistent with a mantle cloud that can be found in "blobs" or "streaks" in the depleted upper mantle and the shallow mantle (the perisphere; Anderson, 1995). Many workers agree that ocean island basalts (OIBs) are commonly derived from low degrees of partial melting of a spinel/garnet peridotite mantle source, while E-MORB is formed from a compositionally similar upper mantle with higher degrees of partial melting (Hofmann and White, 1982; Zindler and Hart, 1986; Hofmann, 1997; Fitton, 2007). OIB and E-MORB commonly occur together in the modern environment, like in Iceland, and can be also found in the

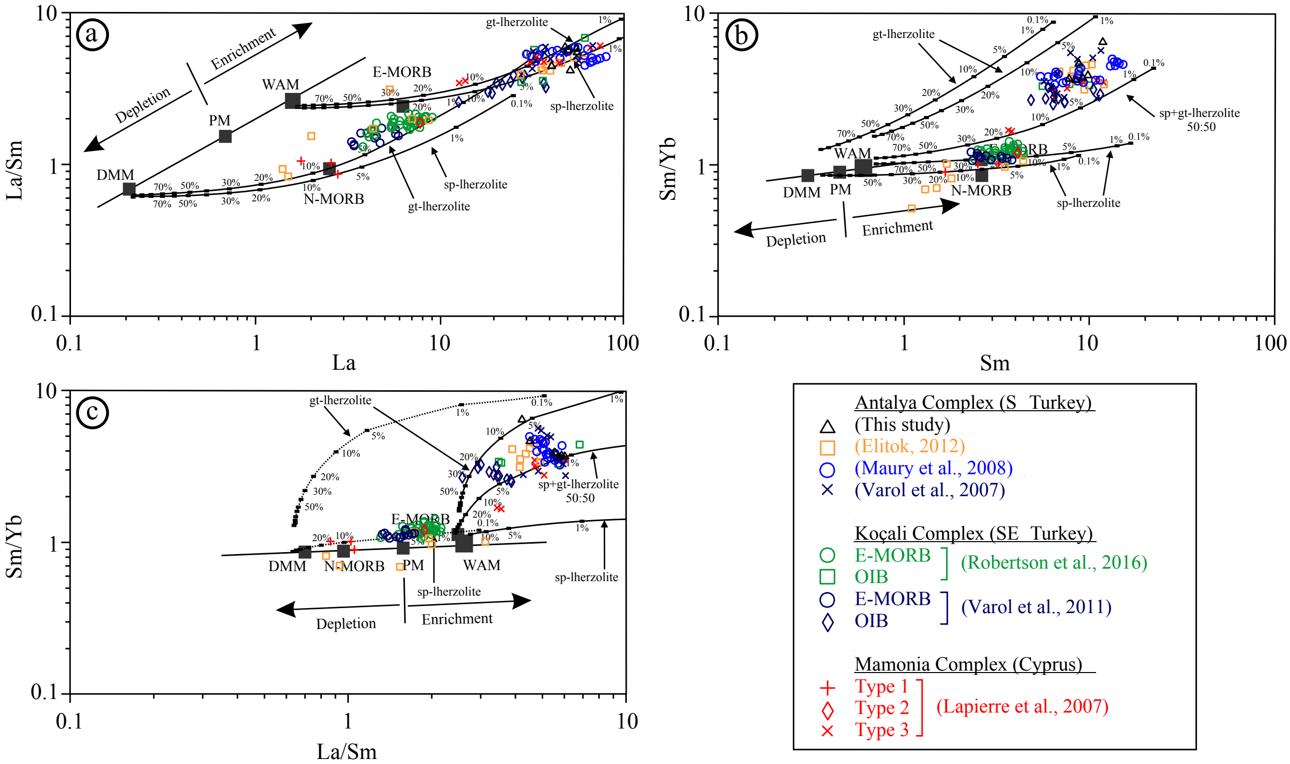

Figure 11. (a) La/Sm vs. La, (b) Sm/Yb vs. Sm, (c) Sm/Yb vs. La/Sm diagrams for the volcanic rocks of Saklıkent (Antalya) region. The modeled melting curves are from Aldanmaz et al. (2000); depleted midocean ridge basalt (MORB) mantle (DMM) is from the compilation of McKenzie and O'Nions (1991, 1995); primitive mantle (PM) composition is from McDonough and Sun (1995); normal MORB (N-MORB), and enriched MORB (E-MORB) compositions are from Sun and McDonough (1989); data for the Western Anatolian Mantle (WAM) fis rom Aldanmaz et al. (2000). The data sources and symbols are the same as in Figure 6.

Tethyan suture zones (Lapierre et al., 2004, 2007; Saccani and Photiades, 2005; Varol et al., 2007, 2011; Aldanmaz et al., 2008; Bagheri and Stampfli, 2008; Maury et al., 2008; Xia et al., 2008; Sayıt et al., 2010; Dai et al., 2011; Elitok, 2012; Robertson et al., 2016).

Late Triassic volcanic rocks of the Eastern Mediterranean region show that there is a close association between E-MORB and OIB, but not N-MORB. It is generally accepted that the widespread presence of Tethyan OIBs has been attributed to a plume-type mantle origin (Dixon and Robertson, 1999; Lapierre et al., 2007; Varol et al., 2007; Maury et al., 2008; Sayıt and Göncüoğlu, 2009; Sayıt, 2013). In contrast, E-MORBs were attributed to the plume-ridge interaction (involving the mixing of the plume-type mantle and depleted MORB source mantle) and the melting of a heterogeneous mantle source (e.g., Aldanmaz et al., 2008; Sayıt and Göncüoğlu, 2009). As seen in the literature, though it is expected that regional-scale uplift remains a significant characteristic for major plume-influenced regions like the Gulf of Aden and East Africa, there is still no evidence to agree with this relationship. However, the relative enrichment instead suggests that there is the availability of a "minor plume", or removal of magma from comparatively enriched "blobs" or "streaks" of the upper mantle (Fitton, 2007). These blobs may have their ultimate origin down in the lower mantle and can be delivered as recycled crustal/mantle materials by means of mantle plumes (e.g., Hofmann and White, 1982; Sun and McDonough, 1989). Geochemically, the coexistence of OIBs and MORBs is the most unambiguous feature for the Mamonia (Cyprus) Complex (Malpas et al., 1993; Lapierre et al., 2007; Chan et al., 2008). The MORB is always known to reflect the early-stage spreading of the Southern Neotethys during Late Triassic time while the OIB is always known to indicate the remnants of Triassic oceanic crust and related seamounts (Lapierre et al., 2007), comparable to the modern southern Red Sea (Robertson, 1990).

The Late Triassic volcanic rocks of the Mamonia Complex are grouped into four rock types based on volcanic eruptions that range from tholeiites to trachytes that have high LREE contents. Figure 13a summarizes the generation of the Mamonia (Cyprus) Complex in southern Neotethys in the Early Triassic (Lapierre et al., 2007). The Mamonia Complex includes the remnants of within-plate oceanic volcanism, situated north of the African-Arabian rifted margin (Figure 13a). Lapierre et al. (2007) suggested

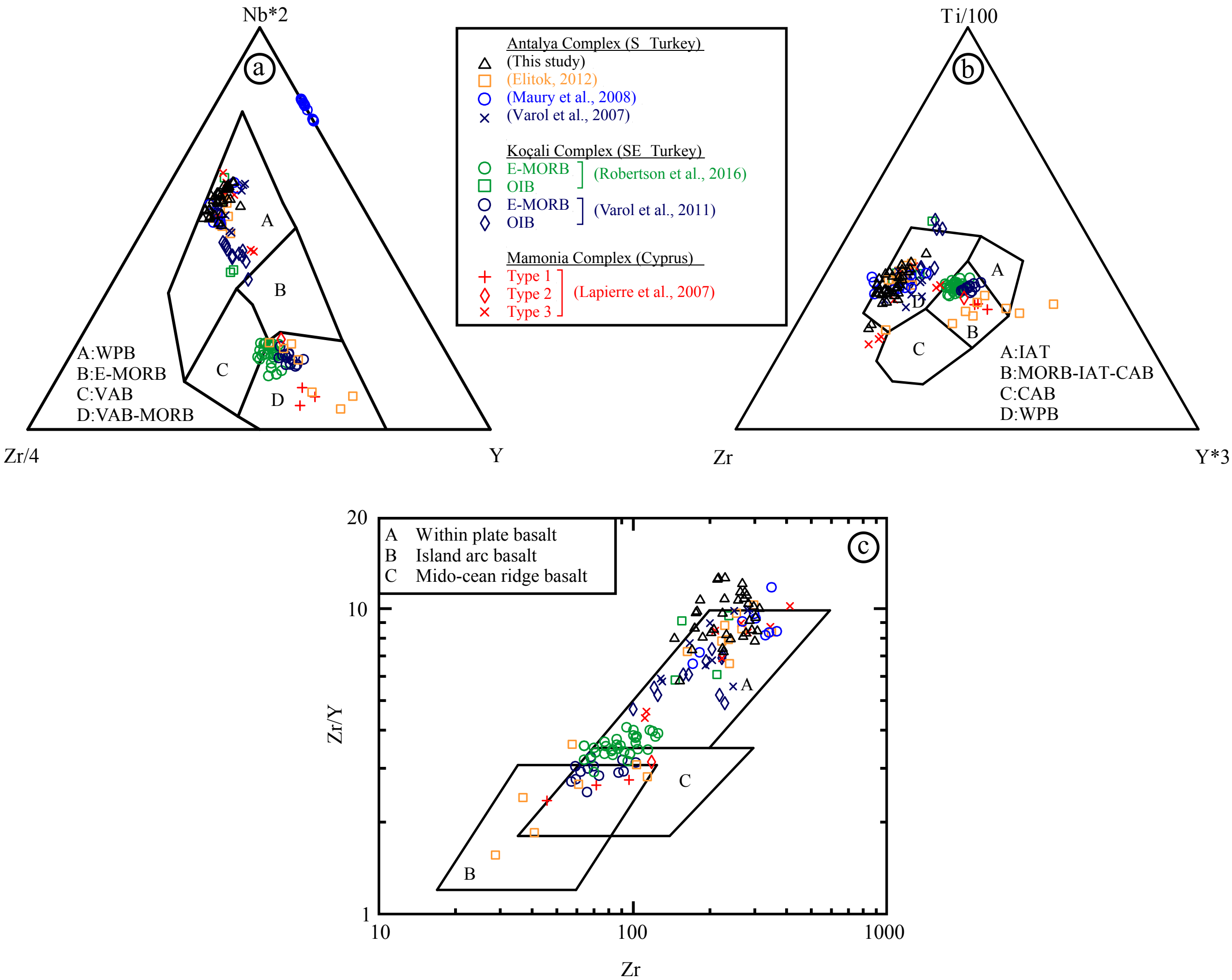

Figure 12. Tectonomagmatic discrimination diagrams for the volcanic rocks of Saklıkent (Antalya) region (a) after Meschede (1986), (b) after Pearce and Cann (1973), and (c) after Pearce & Norry (1979). The data sources and symbols are the same as in Figure 6.

that during the closure of the Southern Neotethyan ocean, deep-basin sedimentary and volcanic rocks of the Mamonia Complex and the Troodos ophiolite were emplaced and reimbricated on the top of the Eratosthenes block during the Maastrichtian.

The volcanic-sedimentary Koçali (Adıyaman) Complex, folded and thrust-imbricated, is composed of lavas, volcaniclastic sediments, pelagic carbonates, radiolarites, manganiferous deposits, and serpentinites (Sungurlu, 1973; Perinçek, 1978, 1979; Fontaine, 1981; Herece, 2008; Yıldırım et al., 2012; Varol et al., 2011; Robertson et al., 2016). Geochemical data presented from the Late Triassic volcanics of the Koçali Complex (Varol et al., 2011; Robertson et al., 2016) suggest that there are two main types of mantle sources for these volcanics. These are (1) E-MORB from the Tarasa Formation and (2) intercalations of OIB and E-MORB from the Konak Formation. The Koçali Complex originated within the continent-ocean transition zone (Figure 13b) (Roberton et al., 2016). Rifted continental margins are classified into two main types: (1) volcanic-rifted margins (e.g., eastern Greenland; Larsen and Saunders, 1998; Fitton et al., 1998, 2000) and (2) nonvolcanic rifted margins (e.g., Iberia-Newfoundland conjugate; Tucholke et al., 2004, 2007). It is documented that most of the Eastern Tethyan rifted margins, including the Koçali Complex, appear to be in an 'intermediate' character between volcanic-rifted margins and the nonvolcanic rifted margins (see Robertson, 2007). Robertson et al. (2016) stated that during the Triassic period, the Tarasa Formations were formed in a distal rifted environment within the outside of the continent-ocean transition zone. The Konak Formation formed in a Red Sea-type small oceanic basin soon after a continental break-up (Figure 13b).

Robertson and Waldron (1990) documented the presence of the Late Triassic basaltic volcanics from the

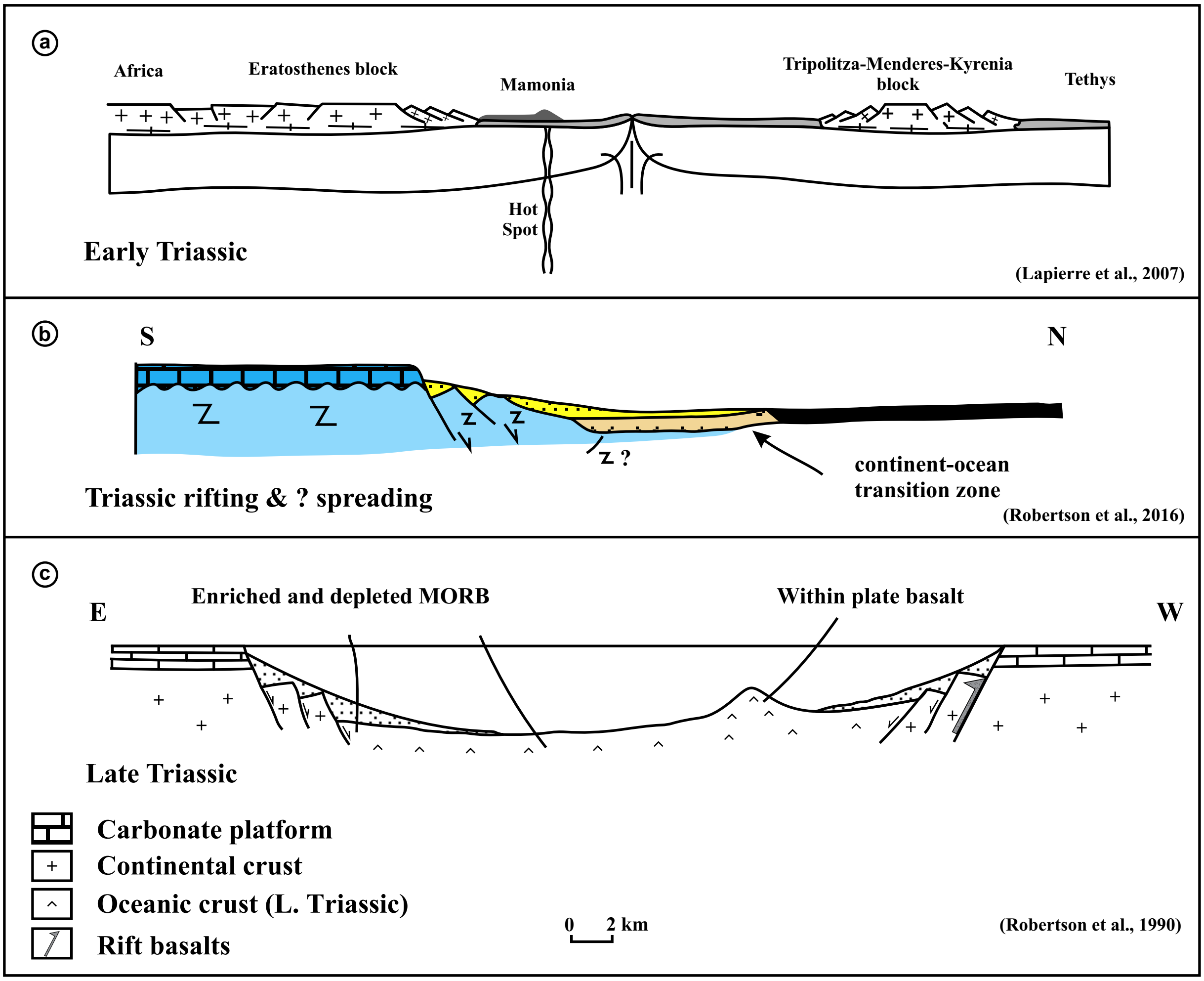

Figure 13. Tectonic models for the genesis of the Late Triassic volcanics (a) from the Mamonia Complex (Lapierre et al., 2007), (b) from the Koçali Complex (Robertson et al., 2016), (c) from the Antalya Complex (Robertson & Waldron 1990). See text for discussion.

Antalya Complex around the margins of the Isparta Angle. The volcanics are observed in close association with radiolarites, hemipelagic Halobia-bearing limestones, turbiditic quartz-bearing sandstones, and reefal limestones. They stated that the geochemistry of the lavas indicates their derivation from within-plate (WP), transitional, and midocean ridge (MOR) type basalts. Robertson and Waldron (1990) indicated that the volcanics are compositionally similar to Late Triassic volcanics in Mamonia (Cyprus) Complex and Oman regions. The volcanics were interpreted to have formed along the margins and basinal facies of a small Red Sea-type oceanic basin (Figure 13c). All the oceanic units were emplaced as a result of subduction/accretion in the Late Cretaceous. Maury et al. (2008) documented the alkaline Late Triassic volcanics from the middle Antalya nappes and concluded that the volcanics do not have evidence from the contribution of continental crust to their genesis and therefore, the lavas occurred in an intraoceanic within-plate plume-related setting. Elitok (2012) documented Late Triassic volcanics from the apex of the Isparta Angle and suggested their genesis within a continental rift basin rather than a true oceanic basin during the Triassic time.

The Neotethys Ocean opened between the north of Arabian and Indian plates during the Middle to Upper Permian, as a result of the break-up of Gondwana (Ricou, 1994; Stampfli and Borel, 2002; Lapierre et al., 2004; Tekin et al., 2019). In southern Turkey, data from Tauride-related units (Mackintosh and Robertson, 2012) show that the rifting started during the Late Permian before extending further during the Early Triassic (Poisson, 1977; Robertson and Woodcock, 1982; Tekin and Sönmez, 2010), while data from the Antalya Complex (Robertson and Woodcock, 1981, 1982; Tekin, 2002a), the Mamonia Complex (Robertson and Woodcock, 1979; Malpas et al., 1993; Chan et al., 2008), and the Koçali Complex

(Robertson et al., 2016) show that the break-up of the continent and the sea-floor spreading all occurred during the Carnian-Norian time.

As indicated above, various oceanic and continental alkaline intraplate alkaline suites were highly associated with a lower mantle-derived plume component by some researchers (Hofmann and White, 1982; Zindler and Hart, 1986; Wilson, 1993). On the other hand, the alkaline volcanics in the Antalya Complex, as well as the Koçali (Adıyaman) and Mamonia (Cyprus) Complexes, might not be explained by a mantle plume component since the alkaline volcanics in the southern Neotethys developed in the rift-related settings and are an extension instead of being related to the plume. A mantle plume would cause a dynamic uplift over a region of approximately 1000–2000 km in diameter (White and McKenzie, 1989). This seems to be unlikely for the southern Neotethyan oceanic basin. On the other hand, apart from the direct involvement of mantle plumes, such materials can be present in the asthenospheric upper mantle as recycled pods/streaks. Thus, as an alternative solution, the idea of a heterogeneous mantle is also suggested (e.g., Aldanmaz et al., 2008; Marroni et al., 2020).

The studied alkaline volcanic rocks in the Saklıkent (Antalya) region, as well as previously published similar volcanics from the Koçali, Antalya, and Mamonia Complexes display OIB-like trace element patterns characterized by enrichment in HFSE, LREE, and MREE, and a slight depletion in HREE relative to N-MORB. The volcanics do not exhibit negative Ta or Nb anomalies. In contrast, the tholeiitic volcanic rocks display E-MORB-like trace element patterns characterized by less enrichment in HFSE, LREE, and MREE compared to alkaline volcanic rocks. Tholeiitic volcanic rocks exhibit a slight negative Ta or Nb anomalies. This evidence suggests that the source region for the alkali basalts has no subduction component, whereas the tholeiitic ones have a slight subduction component.

In summary, the volcanic rocks in the Saklıkent region of the Antalya Complex have alkaline characteristics and were generated by small degrees (~2%–4%) of partial melting of an enriched mantle source relative to the Primitive Mantle (PM) and left a garnet-bearing residue, similar to alkaline volcanics of the Koçali (Adıyaman) and Mamonia (Cyprus) Complexes. In contrast, tholeiitic volcanic rocks were produced by different degrees of partial melting of depleted MORB mantle (DMM) and left a spinel-bearing residue. Geochemical and geological evidence suggests that Late Triassic alkaline and tholeiitic volcanics in Antalya, Mamonia (Cyprus), and Koçali (Adıyaman) Complexes were formed in an extensional environment at the continent-ocean transition zone during rifting of the southern Neotethyan Ocean.

Acknowledgments
We are grateful to Fabio Capponi for performing whole-rock major and trace element analyses and Dr. Pia Voldet for Rare Earth Element (REE) analyses. We are grateful to anonymous referees who made valuable comments and suggestions concerning our manuscript and the editors of Turkish Journal of Earth Sciences.

References

Aldanmaz E, Yalınız MK, Güçtekin A, Göncüoğlu MC (2008). Geochemical characteristics of mafic lavas from the Neotethyan ophiolites in western Turkey: implications for heterogeneous source contribution during variable stages of ocean crust generation. Geological Magazine 145 (1): 37-54.

Aldanmaz E, Pearce JA, Thirlwall MF, Mitchell JG (2000). Petrogenetic evolution of late Cenozoic, post-collision volcanism in western Anatolia, Turkey. Journal of Volcanology and Geothermal Research 102: 67-95.

Al-Riyami K, Robertson AHF, Dixon J, Xenophontos C (2002). Origin and emplacement of the Late Cretaceous Baer-Bassit ophiolite and its metamorphic sole in NW Syria. Lithos 65: 225-260.

Anderson DL (1995). Lithosphere, asthenosphere, and perisphere. Reviews of Geophysics 33 (1): 125-149. doi:10.1029/94RG02785.

Andrew T, Robertson AHF (2002). The Beysehir-Hoyran-Hadim Nappes: genesis and emplacement of Mesozoic marginal and oceanic units of the northern Neotethys in southern Turkey. Journal of the Geological Society London 159 (5): 529-543.

Bagheri S, Stampfli GM (2008). The Anarak, Jandaq and Posht-e-Badam metamorphic complexes in central Iran: New geological data, relationships and tectonic implications. Tectonophysics 451 (1): 123-155.

Ben-Avraham Z, Schattner U, Lazar M, Hall JK, Ben-Gai Y, et al. (2006). Segmentation of the Levant continental margin, eastern Mediterranean. Tectonics 25: TC5002.

Blumenthal MM (1963). Le systéme structural du Taurus sud-Anatolien. In: Durand-Delga M (éditeur) Livre à la Mémoire du Professeur Paul Fallot, consacré à l'évolution paléógéographique et structurale des domaines méditerranéens et alpins d'Europe. Mémoire hors-série de Société Géologique de France, 611-662 (in French).

Bowman S (2011). Regional seismic interpretation of the hydrocarbon prospectivity of offshore Syria. GeoArabia 16 (3): 95-124.

Brunn JH, Dumont JF, Graciansky PC, Gutnic M, Juteau T et al. (1971). Outline of the Geology of the Western Taurids. In: AS Campbell (editor). Geology and History of the Turkey. Petroleum Exploration Society of Libya, Tripoli, pp. 225-255.

Brunn JH, Graciansky PC, Gutnic M, Juteau T, Lefevre R et al. (1970). Structures majeoures et correlationes stratigraphiques dans les Taurides occidentales. Bulletin Société géologique de France 12: 515-524 (in French).

Çelik ÖF, Marzoli A, Marschik R, Chiaradia M (2011). Early-Middle Jurassic intra-oceanic subduction in the İzmir-Ankara-Erzincan ocean, northern Turkey. Tectonophysics 509: 120-134.

Chan GNH, Malpas J, Xenophontos C, Lo CH (2008). Magmatism associated with Gondwanaland rifting and neo-tethyan oceanic basin development: evidence from the Mamonia Complex, SW Cyprus. Journal of the Geological Society London 165: 699-709.

Dai J, Wang C, Hebert R, Li Y, Zhong H, Guillaume R, Bezard R, Wei Y (2011). Late Devonian OIB alkaline gabbro in the Yarlung Zangbo Suture Zone: Remnants of the Paleo-Tethys? Gondwana Research 19: 232-243.

Delaune-Mayère M (1984). Evolution of a Mesozoic passive continental margin: Baer-Bassit (NW Syria). In: Dixon JF, Robertson AHF (editors) The Geological Evolution of the Eastern Mediterranean. Geological Society London Special Publications 151-159.

Dilek Y, Furnes H, Shallo M (2008). Geochemistry of the Jurassic Mirdita ophiolite (Albania) and the MORB to SSZ evolution of a marginal basin oceanic crust. Lithos 100: 174-209.

Dilek Y, Moores EM (1990). Regional tectonics of the eastern Mediterranean ophiolites. In: Malpas J, Moores E, Panayiotou A, Xenophontos C (editors). Proceeding of Troodos Ophiolite Symposium, Cyprus, pp. 295-309.

Dixon JE, Robertson AHF (1999). Are multiple plumes implicated in the Triassic breakup of the Gondwanan margin in the Eastern Mediterranean region? In: Journal of Conference Abstracts 10th European Union of geosciences 4 (1): 314.

Elitok Ö (2012). Geology, geochemistry and geodynamic implications of the mafic-ultramafic rocks from the northern part of the Antalya Complex, SW Turkey. Tectonophysics 568-569: 335-356.

Fitton JG (2007). The OIB paradox. In: Foulger GR, Jurdy DM (editors). Plates, plumes, and planetary processes. Geological Society of America Special Paper 430: 387-412.

Fitton JG, James D, Leeman WP (1991). Basic magmatism associated with the late Cenozoic extension in the western United States: compositional variation in space and time. Journal of Geophysical Research 96: 13693-13711.

Fitton JG, Larsen LM, Saunders AD, Hardarson BS, Kempton PD (2000). Paleogene continental to oceanic magmatism on the SE Greenland continental margin at 63°N: a review of the results of Ocean Drilling Program Legs 152 and 163. Journal of Petrology 41: 951-966.

Fitton JG, Saunders AD, Larsen LM, Hardarson BS, Norry MJ (1998). Volcanic rocks from the southeast Greenland margin at 63°N: Composition, petrogenesis and mantle sources. In: Saunders AD, Larsen HC, Wise SWJr (editors). Proceedings of the Ocean Drilling Program: Scientific Results 152: 331-350.

Fitton JG, Saunders AD, Norry MJ, Hardarson BS, Taylor RN (1997). Thermal and chemical structure of the Iceland plume. Earth and Planetary Science Letters 153: 197-208. doi: 10.1016/S0012-821X (97)00170-2

Floyd PA, Winchester JA (1975). Magma type and tectonic setting discrimination using immobile elements. Earth and Planetary Science Letters 27: 211-218.

Fontaine JK (1981). La plate-forme arabe et sa marge passive au Mésozoique: l'example d'Hazro SE de la Turquie, Thèse 3e cycle, Paris XI (in French).

Göncüoğlu MC (1997). Distribution of Lower Paleozoic units in the Alpine Terranes of Turkey: paleogeographic constraints. In: Göncüoğlu MC, Derman AS (editors). Lower Paleozoic Evolution in northwest Gondwana, Turkish Association of Petroleum Geologists Special Publication 3: pp. 13-24.

Gutnic M, Monod O, Poisson A, Dumont JF (1979). Geologie des Taurides Occidentales (Turquie). Memories Société géologique de France 137: 1-112 (in French).

Hart SR, Erlank AJ, Kable EJD (1974). Sea floor basalt alteration: Some chemical and Sr isotopic effects. Contributions to Mineralogy and Petrology 44: 219-230.

Herece E (2008). Atlas of East Anatolian Fault (EAF). General Directorate of Mineral Research and Exploration Special Publication Series 1-3.

Hofmann AW, White WM (1982). Mantle plumes from ancient oceanic crust. Earth and Planetary Science Letters 57: 421-436.

Hofmann, AW (1997). Mantle geochemistry: The message from oceanic volcanism. Nature 385: 219-229.

Humphris SE, Thompson G (1978). Hydrothermal alteration of oceanic basalts by seawater. Geochimica et Cosmochimica Acta 42: 107-125.

Janney PE, le Roex AP, Carlson RW (2005). Hafnium isotope and trace element constraints on the nature of mantle heterogeneity beneath the central southwest Indian ridge (13°E to 47°E). Journal of Petrology 46: 2427-2464.

Jenkyns HC (1986). Pelagic sediments. In: Reading HG (editor). Sedimentary Environments and Facies. 2nd ed. Oxford, UK: Blackwell.

Jones G, Robertson AHF (1991). Tectono-stratigraphy and evolution of the Mesozoic Pindos Ophiolite and related units, Northwestern Greece. Journal of the Geological Society London 148: 267-288.

Juteau T (1975). Les Ophiolites des Nappes d'Antalya (Taurides Occidentales, Turquie): Petrologie d'un Fragment de I' Ancienne Croute Oceanque Tethysience. Thesis, L'Universite de Nancy I, France (in French).

Juteau T (1980). Ophiolites of Turkey. Ofioliti 2: 199-237.

Juteau T, Whitechurch H (1980). The magmatic cumulates of Antalya (Turkey): evidence of multiple intrusions in an ophiolitic magma chamber. In: Panayiotou A (editor). Proceedings of International Ophiolite Symposium, Geological Survey, Cyprus, pp. 377-391.

Kempton PD, Fitton JG, Hawkesworth CJ, Ormerod DS (1991). Isotopic and trace element constraints on the composition and evolution of the lithosphere beneath the southwestern United States. Journal of Geophysical Research 96: 13713-13735.

Lapierre H, Bosch D, Narros A, Mascle GH, Tardy A et al. (2007). The Mamonia Complex (SW Cyprus) revisited: remnant of Late Triassic intra-oceanic volcanism along the Tethyan southwestern margin. Geological Magazine 144: 1-19.

Lapierre H, Samper A, Bosch D, Maury RC, Bechennec F et al. (2004). The Tethyan plume: geochemical diversity of Middle Permian basalts from the Oman rifted margin. Lithos 74: 167-198.

Larsen HC, Saunders AD (1998). Tectonism and volcanism at the southeast Greenland rifted margin: a record of plume impact and later continental rupture. In: Saunders AD, Larsen HC, Wise S (editors). Proceedings of the Ocean Drilling Program, Scientific Results 152, College Station, Texas (Ocean Drilling Program), 503-534.

le Roux PJ, le Roex AP, Schilling JG, Shimizu N, Perkins WW et al. (2002). Mantle heterogeneity beneath the southern Mid-Atlantic ridge: Trace element evidence for contamination of ambient asthenospheric mantle Earth and Planetary Science Letters 203: 479-498.

Lefèvre R (1967). Un nouvel élément de la géologie du Taurus Lycien: les nappes d'Antalya (Turquie) (in French). A new element of the geology of Lycian Taurus: Antalya nappes (Turkey). Comptes Rendus de l'Académie des Sciences de Paris 165: 1365-1368 (in French).

Mackintosh PW, Robertson AHF (2012). Late Devonian-Late Triassic sedimentary development of the central Taurides, S Turkey: implications for the northern margin of Gondwana. Gondwana Research 21: 1089-1114.

Malpas J, Calon T, Squires G (1993). The development of a Late Cretaceous microplate suture zone in SW Cyprus. In: Prichard HM, Alabaster T, Harris NBW, Neary CR (editors). Magmatic processes and plate tectonics. Geological Society London Special Publications 76: pp. 177-195.

Marcoux J (1995). Initiation of the south-Neotethys margin in the Antalya nappes (SW Turkey): Late Permian and Early Mid-Triassic rifting events, Late Mid-Triassic oceanization. EGU Abstracts 7: 175.

Marroni M, Göncüoglu MC, Frassi C, Sayıt K, Pandolfi L et al. (2020). The Intra-Pontide ophiolites in northern Turkey revisited: from birth to death of a Neotethyan oceanic domain. Geoscience Frontiers 11: 129-149.

Maury RC, Lapierre H, Bosch D, Marcoux J, Krystyn L et al. (2008). The alkaline intraplate volcanism of the Antalya nappes (Turkey): a Late Triassic remnant of the Neotethys. Bulletin de la Société géologique de France 179 (4): 397-410.

McDonough WF, Sun SS (1995). The composition of the Earth. Chemical Geology 120: 223-253.

McKenzie DP, O'Nions RK (1991). Partial melt distributions from inversion of rare earth element concentrations. Journal of Petrology 32: 1021-1091.

McKenzie DP, O'Nions RK (1995). The source regions of ocean island basalts. Journal of Petrology 36: 133-159.

Meschede M (1986). A method of discriminating between different types of mid-ocean ridge basalts and continental tholeiites with the Nb-Zr-Y diagram. Chemical Geology 56: 207-218.

MTA (2000). 1/100.000 scale Turkish Geology Maps, Antalya 024 sheet. General Directorate of Mineral Research and Exploration, Ankara (in Turkish).

Murton BJ, Tindle AG, Milton JA, Sauter D (2005). Heterogeneity in southern central Indian ridge MORB: Implications for ridge–hot spot interaction: Geochemistry Geophysics Geosystems 6: Q03E20.

Nauret F, Abouchami W, Galer SJG, Hofmann AW, Hémond C et al. (2006). Correlated trace element-Pb isotope enrichments in Indian MORB along 18–20°S, Central Indian Ridge Earth and Planetary Science Letters 245: 137–152.

Özgül N (1976). Some Geological Aspects of the Taurus Orogenic Belt (Turkey). Geological Society of Turkey Bulletin 19: 65-78 (in Turkish with English Abstract).

Özgül N (1984). Stratigraphy and Tectonic Evolution of the Central Taurides. In: Tekeli O, Göncüoğlu MC (editors). Geology of the Taurus Belt. Proceedings of International Symposium, Ankara. pp. 77-90.

Özgül N, Arpat E (1973). Structural units of the Taurus orogenic belt and their continuation in neighbouring regions: selection of papers on the Eastern Mediterranean region. Presented at 23rd congress of CIESM in Athens. Bulletin of the Geological Society Greece 10 (1): 156-164.

Özgül, N (1971). Orta Torosların kuzey kesiminin yapısal gelişiminde blok hareketlerin önemi. Türkiye Jeoloji Kurumu Bülteni 14: 75-87 (in Turkish).

Parlak O, Rızaoğlu T, Bağcı U, Karaoğlan F, Höck V (2009). Tectonic significance of the geochemistry and petrology of ophiolites in southeast Anatolia, Turkey. Tectonophysics 473 (1–2): 173-187.

Parlak O, Robertson, AHF (2004). Tectonic Setting and Evolution of the Ophiolite-Related Mersin Mélange, Southern Turkey: Its Role in the Tectonic-Sedimentary Setting of the Tethys in the Eastern Mediterranean Region. Geological Magazine 141: 257-286.

Pearce JA (1983). Role of the sub-continental lithosphere in magma genesis at active continental margins. In: Hawkesworth CJ, Norry MJ (editors). Continental Basalts and Mantle Xenoliths, Shiva, Nantwich, pp. 230-249.

Pearce JA (1996). A user's guide to basalt discrimination diagrams. In: Wyman DA (editor) Trace Element Geochemistry of Volcanic Rocks: Applications for Massive Sulphide Exploration. Geological Association of Canada, Short Course Notes 12: pp. 79-113.

Pearce JA (2008). Geochemical fingerprinting of oceanic basalts with applications to ophiolite classification and the search for Archean oceanic crust. Lithos 100: 14-48.

Pearce JA, Cann JR (1973). Tectonic setting of basaltic volcanic rocks determined using trace element analysis. Earth and Planetary Science Letters 19: 290-300.

Pearce JA, Norry MJ (1979). Petrogenetic implications of Ti, Zr, Y, and Nb variations in volcanic rocks. Contributions to Mineral and Petrology 69: 33-47.

Pearce JA, Peate DW (1995). Tectonic implications of the composition of volcanic arc lavas. Annual Review of Earth and Planetary Sciences 23: 251-285.

Pe-Piper G (1982). Geochemistry, tectonic setting and metamorphism of the mid-Triassic volcanic rocks of Greece. Tectonophysics 85: 23-272.

Perinçek D (1978). Geological investigation and petroleum prospects of the region between Çelikhan-Sincik-Kocali (city of Adıyaman). PhD, Istanbul University and TPAO Report No 1250 (in Turkish).

Perinçek D (1979). Geological investigation of the Çelikhan-Sincik-Koçali area (Adıyaman province). Revue de la Faculté des Sciences de l'Université d'İstanbul B44, 127-147.

Perinçek D (1980). Bitlis metamorfitlerinde volkanitli Triyas. Türkiye Jeoloji Kurumu Bülteni 23: 201-211 (in Turkish).

Poisson A (1977). Récherches géologiques dans les Taurides occidentales, Turquie. PhD, University of Paris-Sud, Orsay, France.

Poisson A (1984). The extension of the Ionia trough into southwestern Turkey. In: Dickson JE, Robertson AHF (editors). Geological Evolution of the Eastern Mediterranean. Geological Society of London Special Publications 17: pp. 241-250.

Ricou LE (1994). Tethys reconstructed: plates, continental fragments and their boundaries since 260 Ma from Central America to south-eastern Asia. Geodinamica Acta 7: 169-218. doi: 10.1080/09853111.1994.11105266

Ricou LE, Marcoux J, Whitechurch H (1984). The Mesozoic organization of the Taurides: one or several ocean basins? In: Dixon JE, Robertson AHF (editors). The Geological Evolution of the Eastern Mediterranean. Geological Society London Special Publications 17: pp. 349-359. doi: 10.1144/GSL.SP.1984.017.01.25

Roberts G, Pearce D (2007). Hydrocarbon plays and prospectivity of the Levantine Basin, offshore Lebanon and Syria from modern seismic data. GeoArabia 12 (3): 99-124.

Robertson AHF (1990). Tectonic evolution of Cyprus. In: Malpas J, Moores EM, Panayiotou A, Xenophontos C (editors). Ophiolites-Oceanic Crustal Analogues. Proceedings of the International Symposium 'Troodos 1987' Geological Survey Department, Cyprus. pp. 235-253.

Robertson AHF (1993). Mesozoic-Tertiary sedimentary and tectonic evolution of Neotethyan carbonate platforms, margins and small ocean basins in the Antalya Complex, S.W. Turkey. In: Frostick LE, Steel R (editors). Tectonic Controls and Signatures in Sedimentary Successions. Special Publication of the International Association of Sedimentologists 20: pp. 415-465.

Robertson AHF (1998). Mesozoic-Tertiary tectonic evolution of the easternmost Mediterranean area: integration of marine and land evidence. In: Robertson AHF, Emeis KC, Richter C, Camerlenghi A (editors). Proceedings of the Ocean Drilling Program, Scientific Results 160: pp. 723-782.

Robertson AHF (2002). Overview of the genesis and emplacement of Mesozoic ophiolites in the Eastern Mediterranean Tethyan region. Lithos 65: 1-67.

Robertson AHF (2007). Overview of tectonic settings related to the rifting and opening of Mesozoic ocean basins in the Eastern Tethys: Oman, Himalayas and Eastern Mediterranean regions. In: Karner G, Manatschal G, Pinheiro LM (editors). Imaging, Mapping and Modelling Continental Lithosphere Extension and Breakup. Geological Society London Special Publications 282: pp. 325-389.

Robertson AHF (2012). Tectonic development of Greece and Albania in the context of alternative reconstructions of Tethys in the Eastern Mediterranean region during Late Palaeozoic-Cenozoic time. International Geology Review 54: 373-454.

Robertson AHF, Dixon JD (1984). Introduction: Aspects of the Geological Evolution of the Eastern Mediterranean. In: Dixon JE, Robertson AHF (editors). The Geological Evolution of the Eastern Mediterranean. Geological Society London, Special Publications pp. 17: 1-74.

Robertson AHF, Karamata S (1994). The role of subduction–accretion processes in the tectonic evolution of the Mesozoic Tethys in Serbia. Tectonophysics 234: 73-94.

Robertson AHF, Parlak O, Ustaömer T (2012). Overview of the Palaeozoic-Neogene evolution of Neotethys in the Eastern Mediterranean region (S Turkey, Cyprus, Syria). Petroleum Geoscience 18: 381-404.

Robertson AHF, Parlak O, Yıldırım N, Dumitrica P, Taslı K (2016). Late Triassic rifting and Jurassic? Cretaceous passive margin development of the Southern Neotethys: evidence from the Adıyaman area, SE Turkey. International Journal of Earth Sciences 105: 167-201.

Robertson AHF, Ustaömer T, Pickett EA, Collins AS, Andrew T et al. (2004). Testing models of Late Palaeozoic-Early Mesozoic orogeny in Western Turkey: support for an evolving open-Tethys model. Journal of the Geological Society London 161: 501-511.

Robertson AHF, Waldron JWF (1990). Geochemistry and tectonic setting of Late Triassic and Late Jurassic-Early Cretaceous basaltic extrusives from the Antalya Complex, south west Turkey. In: Savaşçın MY, Eronat AH (editors). Proceedings of the International Earth Sciences Congress on Aegean Regions, Dokuz Eylül University, İzmir. 2: pp. 279-299.

Robertson AHF, Woodcock NH (1979). The Mamonia Complex, SW Cyprus: the evolution and emplacement of a Mesozoic continental margin. Geological Society of America Bulletin 90: 651-665.

Robertson AHF, Woodcock NH (1980). Tectonic setting of the Troodos massif in the East Mediterranean. In: Ophiolites, Panayiotou A (editor). Geological Survey Department, Cyprus. pp. 36-49.

Robertson AHF, Woodcock NH (1981) Gödene Zone, Antalya Complex, SW Turkey: volcanism and sedimentation on Mesozoic marginal ocean crust. Geologisches Rundschau 70: 177-1214.

Robertson AHF, Woodcock NH (1982). Sedimentary history of the southwestern segment of the Mesozoic-Tertiary Antalya continental margin, southwestern Turkey. Eclogae Geologicae Helvetica 75: 517-562.

Rudnick RI, Barth M, Horn I, McDonough WF (2000). Rutile-bearing eclogites: missing link between continents and depleted mantle. Science 287: 278-281.

Saccani E, Photiades A (2005). Petrogenesis and tectonomagmatic significance of volcanic and subvolcanic rocks in the Albanide-Hellenide ophiolitic mélanges. The Island Arc 14: 494-516

Sayıt K (2013). Immobile trace element systematics of oceanic island basalts: the role of oceanic lithosphere in creating the geochemical diversity. Ofioliti 38: 101-120.

Sayıt K, Göncüoğlu MC (2009). Geochemistry of mafic rocks of the Karakaya Complex, Turkey: Evidence for plume-involvement in the extensional oceanic regime during Middle-Late Triassic. International Journal of Earth Sciences 98: 367-385.

Sayıt K, Göncüoglu MC, Furman T (2010). Petrological reconstruction of Triassic seamounts/oceanic islands within the Palaeotethys: Geochemical implications from the Karakaya subduction/accretion Complex, Northern Turkey. Lithos 119: 501-511.

Şenel M (1997). 1/100.000 scale geological maps of Turkey, Antalya M10, M11, L10, L11 and L12 quadrangles. General Directorate of Mineral Research and Exploration, Ankara, Turkey (in Turkish).

Şenel M, Dalkılıç H, Gedik I, Serdaroğlu M, Bölükbaşı S et al. (1992). Egirdir-Yenişarbademli-Gebiz ve Geriş-Köprülü (Isparta-Antalya) arasında kalan alanların jeolojisi. General Directorate Mineral Research Exploration Institute, Report No 9390, 559 pp. (unpublished) (in Turkish).

Şenel M, Gedik I, Dalkılıç H, Serdaroğlu M, Bilgin AZ et al. (1996). Isparta büklümü doğusunda, otokton ve allokton birimlerin stratigrafisi (Batı Toroslar). Bulletin of Mineral Research and Exploration Institute, Turkey 118: 111-160 (in Turkish).

Şenel M, Kengil R, Ünverdi M, Gözler MZ, Serdaroglu M (1981). Teke Torosları guneydogusunun jeolojisi. Bulletin of Mineral Research and Exploration Institute, Turkey 95/96: 13-43.

Şengör AMC, Yılmaz Y (1981). Tethyan evolution of Turkey, a plate tectonic approach. Tectonophysics 75: 181-241.

Shallo M, Kodra A, Gjata K (1990). Geotectonics of the Albanian ophiolites. In: Malpas J, Moores EM, Panayiotou A, Xenophontos C (editors). Ophiolites: Oceanic Crustal Analogues. The Geological Survey Department, Cyprus, pp. 265-270.

Stampfli GM, Borel DG (2002). A plate tectonic model for the Paleozoic and Mesozoic constrained by dynamic plate boundaries and restored synthetic oceanic isochrones. Earth Planetary Science Letters 196: 17-33.

Sun SS, McDonough WF (1989). Chemical and isotopic systematics of ocean basalts: Implications for mantle composition and processes. In: Saunders AD, Norry MJ (editors). Magmatism in the Ocean Basins. Geological Society London Special Publication 42: pp. 313-345.

Sungurlu O (1972). Geology between Gölbaşı-Gerger Fields, VI. Region, TPAO Report, No 802, unpublished (in Turkish).

Tatsumi Y, Eggins S (1995). Subduction Zone Magmatism Boston, Blackwell Sci., 211 p.

Tekin UK (2002). Late Triassic (Late Norian-Rhaetian) radiolarians from the Antalya Nappes, Central Taurides, Southern Turkey. Rivista Italiana di Paleontologia e Stratigrafia 108: 415-440.

Tekin UK, Okuyucu C, Sayıt K, Bedi Y, Noble PJ et al. (2019). Integrated Radiolaria, benthic foraminifera and conodont biochronology of the pelagic Permian blocks/tectonic slices and geochemistry of associated volcanic rocks from the Mersin Mélange, southern Turkey: implications for the Permian evolution of the northern Neotethys. The Island Arc 28 (2): 1-36.

Tekin UK, Sönmez I (2010). Late Ladinian radiolarians from the Tahtalidag Nappe of the Antalya nappes, SW Turkey: remarks on the late Middle and Late Triassic evolution of the Tahtalıdağ Nappe. Acta Geologica Polonica 60: 199-217.

Tucholke BE, Sawyer DS, Sibuet J-C (2007). Breakup of the Newfoundland-Iberia rift. In: Karner GD, Manatschal G, Pinheiro LM (editors). Imaging, Mapping and Modelling Continental Lithosphere Extension and Breakup. Geological Society London Special Publications 282: pp. 9-45.

Tucholke BE, Sibuet J-C, Klaus A (2004). Proceedings of the Ocean Drilling Program, Initial Reports 210, College Station, Texas (Ocean Drilling Program), 78 pp.

Uzunçimen S, Tekin UK, Bedi Y, Perinçek D, Varol E, Soycan H (2011). Discovery of the Late Triassic (Middle Carnian-Rhaetian) radiolarians in the volcano-sedimentary sequences of the Koçali Complex, SE Turkey: correlation with the other Tauride units. Journal of Asian Earth Sciences 40: 180-200.

Varol E, Bedi Y, Tekin UK, Uzunçimen S (2011). Geochemical and petrological characteristics of Late Triassic basic and volcanic rocks from the Koçali Complex, SE Turkey: implications for the Triassic evolution of Southern Tethys. Ofioliti 36: 101-115.

Varol E, Tekin UK, Temel A (2007). Dating and geochemical properties of middle to late Carnian basalts from the Alakırçay Nappe of the Antalya Nappes, SW Turkey: Implications for the evolution of southern branch of Neotethys. Ofioliti 32 (2): 163-176.

Waldron JWF (1984). Structural history of the Antalya Complex in the Isparta angle, Southwest Turkey. In: Dixon JE, Robertson AHF (editors). The Geological Evolution of the Eastern Mediterranean, Geological Society of London Special Publication 17: pp. 273-286.

White WM, McKenzie DP (1989). Magmatism at rift zones: the generation of volcanic continental margins and flood basalts. Journal of Geophysical Research 94: 7685-7729.

Whitney DL, Evans BW (2010). Abbreviations for names of rock-forming minerals. American Mineralogist 95: 185-187.

Wilson M (1993). Geochemical characteristics of oceanic and continental basalts: a key to mantle dynamics? Journal of the Geological Society, London 150: 977-990.

Woodcock NH, Robertson AHF (1977). Wrench and thrust tectonics along a Mesozoic-Cenozoic continental margin: Antalya Complex, SW Turkey. Journal of the Geological Society London 139: 147-163.

Woodcock NH, Robertson AHF (1982). Wrench and thrust tectonics along a Mesozoic Cenozoic continental margin: Antalya Complex, SW Turkey. Journal of the Geological Society London 193: 147-163.

Xia B, Chen G-W, Wang R, Wang Q (2008). Seamount volcanism associated with the Xigaze ophiolite, Southern Tibet. Journal of Asian Earth Sciences 32: 396-405.

Yıldırım N, Parlak O, Robertson AHF (2012). Geochemistry and tectonıc significance of the Koçali ophiolite and the related Koçali melange, Adıyaman region, SE Turkey. 65. Türkiye Jeoloji Kurultayı, 2-7 Nisan 2012, Ankara, pp. 82-83.

Yılmaz PO (1984). Fossil and K-Ar data for the age of the Antalya complex, SW Turkey. In: Dixon JA, Robertson AHF (editors). The Geological Evolution of the Eastern Mediterranean. Geological Society of London Special Publication 17: pp. 335-347.

Zindler A, Hart S (1986). Chemical geodynamics. Annual Review of Earth and Planetary Sciences 14: 493-571.